



KTH Architecture and
the Built Environment

*Block stability analysis using
deterministic and probabilistic methods*

Mehdi Bagheri

Doctoral Thesis

Division of Soil and Rock Mechanics

Department of Civil and Architectural Engineering

Royal Institute of Technology

Stockholm, 2011

TRITA-JOB PHD 1016

ISSN 1650-9501

Acknowledgements

The study was initiated and supervised by Professor Håkan Stille and conducted at the Division of Soil and Rock Mechanics at the Royal Institute of Technology.

The Swedish Rock Engineering Research Foundation (BeFo) provided financial support for the project.

I would like to thank all those who made this research possible. Special thanks go to Professor Håkan Stille for his fruitful discussions and unwavering encouragement. I must mention that, without his help and support, this research would not have been possible. I am therefore deeply indebted to him. I would like to thank my friend, Alireza Baghbanan, faculty member of Isfahan University of Technology for his cooperation in producing in some papers. I also wish to thank Tomas Franzén and Mikael Hellsten for their interest in the project. I want to thanks Eva Friedman from BeFo. I am grateful to the reference group for their comments and discussions, which made this work better. I extend my great appreciation to Beatrice Lindstrom from Golder Associates, Mats Holmberg from Tunnel Engineering, Rolf Christiansson from SKB, Jimmy Toyra and Thomas Dalmalm from the Swedish Transport Administration, Jonny Sjöberg, Erling Nordlund and Kelvis Prez from LTU, and Lars O Ericksson and Mirijam Zetterlund from Chalmers University of Technology. I am also extremely grateful to Mark Christianson from Itasca Consulting Group. I want to thank Susan Long for English corrections. My gratitude goes to all my colleagues at the Division of Soil and Rock Mechanics, especially Sofia Jonsson and Lena Wennerlund. Finally, special thanks go to my fair lady, Sareh, who stuck with me throughout my work on the thesis. In the end, her support and encouragement made this thesis possible.

Abstract

This thesis presents a discussion of design tools for analysing block stability around a tunnel. First, it was determined that joint length and field stress have a significant influence on estimating block stability. The results of calculations using methods based on kinematic limit equilibrium (KLE) were compared with the results of filtered DFN-DEM, which are closer to reality. The comparison shows that none of the KLE approaches—conventional, limited joint length, limited joint length with stress and probabilistic KLE – could provide results similar to DFN-DEM. This is due to KLE's unrealistic assumptions in estimating either volume or clamping forces.

A simple mechanism for estimating clamping forces such as continuum mechanics or the solution proposed by Crawford-Bray leads to an overestimation of clamping forces, and thus unsafe design. The results of such approaches were compared to those of DEM, and it was determined that these simple mechanisms ignore a key stage of relaxation of clamping forces due to joint existence. The amount of relaxation is a function of many parameters, such as stiffness of the joint and surrounding rock, the joint friction angle and the block half-apical angle.

Based on a conceptual model, the key stage was considered in a new analytical solution for symmetric blocks, and the amount of joint relaxation was quantified. The results of the new analytical solution compared to those of DEM and the model uncertainty of the new solution was quantified.

Further numerical investigations based on local and regional stress models were performed to study initial clamping forces. Numerical analyses reveal

that local stresses, which are a product of regional stress and joint stiffness, govern block stability. Models with a block assembly show that the clamping forces in a block assembly are equal to the clamping forces in a regional stress model. Therefore, considering a single block in massive rock results in lower clamping forces and thus safer design compared to a block assembly in the same condition of in-situ stress and properties.

Furthermore, a sensitivity analysis was conducted to determine which is the most important parameter by assessing sensitivity factors and studying the applicability of the partial coefficient method for designing block stability.

It was determined that the governing parameter is the dispersion of the half-apical angle. For a dip angle with a high dispersion, partial factors become very large and the design value for clamping forces is close to zero. This suggests that in cases with a high dispersion of the half-apical angle, the clamping forces could be ignored in a stability analysis, unlike in cases with a lower dispersion. The costs of gathering more information about the joint dip angle could be compared to the costs of overdesign. The use of partial factors is uncertain, at least without dividing the problem into sub-classes. The application of partial factors is possible in some circumstances but not always, and a FORM analysis is preferable.

Key words: Block stability analysis, Model uncertainty, Joint relaxation, Partial factor, Sensitivity analysis

Sammanfattning

I denna avhandling diskuteras de olika designverktøyen för blockstabilitetsanalys. Undersökningarna i denna avhandling visar att sprickors längd och spänning spelar stor roll när man ska bedöma instabila blockvolymmer. Resultaten från KLE jämfördes med de mer verklighetstroga resultaten från DFN-DEM, och jämförelserna visade att ingen av KLE metoderna är kapabla att bedöma oastabila blockvolymmer på ett verklighetstroget sätt. Detta beror på orealistiska antaganden för blockvolymbedömning eller klämkrakter.

Enkla mekanismer som kontinuum metoder eller Crawford-Bray överskattar klämkrakterna och ger därför en osäker design. Jämförelser mellan resultaten från Crawford-Bray och DEM visar att ett viktigt steg, nämligen relaxationen av klämkrakter p.g.a. sprickor, inte har inkluderats i den analytiska lösningen. Storleken på relaxationen beror på olika parameter, bl.a. styvheten hos både sprickor och bergmassan, friktionsvinkel och toppvinkeln. Baserad på en begreppsmässig modell hensyn togs till nyckel steget i en ny analytisk lösning för symmetriska block. Och storleken på sprickrelaxationen kvantifierades. Resultaten från den nya modellen och DEM jämfördes med och modellosäkerheten för den nya lösningen bedömdes.

Ytterligare numeriska modeller baserade på lokala och regionala spänningsmodeller gjordes för att studera de initiala klämkrakterna. Modellerna visar att den lokala spänningen, vilken är ett resultat av den regionala spänningen och sprickors styvhet, styr blockstabiliteten.

Modellen för en blocksamling visar att klämkrafterna på enskilda block är mindre än klämkrafterna på en blocksamling och därför är en design baserad på enskilda block ett säkrare val.

Vidare så gjordes det även en känslighetsanalys för att bedöma vilken parameter påverkar designen mest och om partiella koefficienter är användbara eller ej.

Det visade sig att spridningen hos toppvinkeln är den parameter som styr mest. En stor osäkerhet för toppvinkeln leder till att de partiella koefficienterna för klämkrafterna blir för höga och detta minskar deras designvärde. Detta betyder att klämkrafterna inte bidrar till stabiliteten eftersom de minskar med stora osäkerheter hos toppvinkel, däremot bör de räknas in för de fall där toppvinkeln har en mindre osäkerhet. Avslutningsvis så kan man påstå att kostnaderna för bergsförstärkning kan jämföras med kostnaderna för insamling av information för toppvinkeln, och att användningen av partiella koefficienter leder till osäkra resultat för vissa fall och bör därför ersättas med FORM.

List of Publications

This thesis incorporates four journal articles and one conference paper:

Journal articles

- **Paper I**, Nord, G. Bagheri, M. Baghbanan, A. Stille, H. Design consideration of large caverns by using advanced drilling equipment, *Felsbau*, Vol 25 (5) P 131-136, 2007.
- **Paper II**, Bagheri, M. Stille, H. Investigation of model uncertainty for block stability analysis, *Int. J. Numerical and analytical in geomechanics*, Vol 35 (7) P 824-836, 2011.
- **Paper III**, Bagheri, M. Stille, H. A new analytical solution based on joint relaxation for analysing symmetrical block stability, *Int. J. Numerical and analytical in geomechanics*, Doi 10.1002/nag.1119, 2011.
- **Paper IV**, Bagheri, M. Stille, H. Application of partial factors to block stability analysis, to be submitted to *International journal of Georisk*.

Conference paper with peer review

- **Paper V**, Bagheri, M. Baghbanan, A. Stille, H. Some aspects on model uncertainty in the calculation of block stability using kinematic limit equilibrium, ARMA, 42nd US Rock Mechanics -2nd US-Canada Rock Mechanics Symposium, American Rock Mechanics Association, San Francisco, California, 2008.

Contents

Chapter 1 Introduction-----	1
1.1 History and background-----	1
1.2 Uncertainty-----	1
1.3 Safety and economy -----	2
1.4 Objectives -----	3
1.5 Limitations -----	3
1.6 Structure of the thesis-----	4
Chapter 2 Review and discussion of today's design tools -----	7
2.1 Introduction -----	7
2.2 Block stability -----	7
2.3 Application of today's design tools (a case study) -----	10
2.3.1 Introduction-----	10
2.3.2 KLE approach-----	11
2.3.3 DFN calibration-----	12
2.3.4 DFN-DEM approach-----	14
2.3.5 Results of applying design tools-----	16
2.4 Discussion-----	18
2.5 Summary and conclusion -----	20
Chapter 3 Analytical methods based on joint relaxation -----	23
3.1 Introduction and history-----	23

3.2 Crawford-Bray solution-----	23
3.3 Initial clamping forces-----	24
3.4 Model uncertainty of the Crawford-Bray solution-----	27
3.4.1 Methodology to assess model uncertainty-----	27
3.4.2 Results of simulations-----	29
3.4.3 Reasons for model uncertainty-----	31
3.4.4 Summary and conclusions of the Crawford-Bray solution-----	34
3.5 New conceptual model -----	34
3.6 New analytical solution -----	36
3.7 Verification of clamping forces calculated in a discontinuous medium -----	38
3.8 Ultimate pull-out force and model uncertainty calculation using the new solution -----	40
3.9 Conclusion -----	42
Chapter 4 Application of partial factors to block stability analysis-----	45
4.1 Introduction -----	45
4.2 Methodology and assumptions -----	45
4.3 Ultimate limit state function -----	46
4.3.1 Block stability ultimate limit state function-----	46
4.3.2 Joint stiffness-----	48
4.3.3 Ratio of joint stiffness-----	49

4.3.4 Summary of ultimate limit state function and its variables-----	50
<i>Ultimate state function</i> -----	50
<i>Variables</i> -----	50
4.4 FORM analysis-----	51
4.4.1 Inputs-----	51
<i>Coefficient A</i> -----	51
<i>Friction angle</i> -----	51
<i>Half-apical angle</i> -----	52
<i>Model uncertainty</i> -----	52
<i>Normal force</i> -----	52
<i>Normal force reduction</i> -----	53
4.4.2 Correlation coefficient-----	56
4.5 Results and summary of FORM analyses -----	56
4.5.1 Introduction-----	56
4.5.2 Critical sensitivity factors-----	56
4.6 Comparison between partial factors and FORM-----	58
4.6.1 Partial factors and their application-----	58
4.6.2 Partial factors for a shallow depth tunnel-----	59
4.7 Discussion and conclusion -----	61
Chapter 5 Discussion and conclusion-----	63

5.1 Introduction -----	63
5.2 Summary -----	63
5.3 Conclusion -----	64
5.4 Suggestions to the designer -----	66
5.5 Further research-----	66
References-----	67
Appended papers	

Chapter 1 Introduction

1.1 History and background

Block failure is a common failure mode in tunnels, and there are many published international reports on the subject (see, for example, Hoek and Brown, 1980; Goodman and Shi, 1985; Åkesson, 1985; and Sjöström, 1989). Many articles have also been published in Sweden (see, for example, Morfeldt, 1973; Krauland, 1975; Hedlund et al., 1980; Bergman, 1985; Benedik, 1987; Hansen, 1989; Olsson and Stille, 1989; and Sundel, 1991).

While extensive research has been carried out to analyse block stability (for example, Crawford Bray, 1983; Sofianos, 1984, 1986; Elsworth, 1986; Mauldon, 1995; Nomikos et al., 1999; and Nomikos et al., 2002, 2006, 2008), block failure is still an issue in tunnelling. This is due to the complexities of the block stability problem and the uncertainties involved in the design.

1.2 Uncertainty

Generally after the block volume is determined, a stability analysis of the block is performed using mechanical models. In this design process, three types of uncertainties – parameter uncertainty, model uncertainty and geometrical uncertainty – are involved. These uncertainties influence the safety and economy of the rock support installed.

Parameter uncertainty exists in mechanical parameters (joint stiffness, friction angle etc.). Uncertainties in estimating block geometry entail uncertainties about the localisation of joints, their length, orientation and length. The main source of parameter and geometrical uncertainty is the

limitations of field investigations. Field investigations of joint length and orientation are subject to uncertainty because data are obtained from a two-dimensional surface of boreholes or pilot tunnels without any access to the third dimension, which is hidden behind the rock surface.

Uncertainties in the mechanical properties of joints such as joint friction, cohesion and stiffnesses arise because of a lack of knowledge about and limitations on the possibilities of carrying out large-scale in-situ tests.

There are also uncertainties in the design tools used to estimate block volume and solve for equilibrium. Every design tool is based on simplifications so there is model uncertainty associated with the use of each one. The designer must be aware of the weaknesses and model uncertainty of these design tools.

1.3 Safety and economy

Design based on the safety factor is applied in practice to block stability analyses, but the failure of blocks is still observed because of existing uncertainties. However, use of a higher safety factor may lead to the uneconomical design of tunnels and still may not provide a safer design. This suggests that the safety factor does not visualise the uncertainties in the design of a block, so other methods must be applied which take into account the uncertainties.

New codes, such as Eurocode (EN, 1997), recommend the use of limit state design and propose to quantify the uncertainties by applying partial factors. However, no report discussing the use of partial factors for block stability analysis in tunnels has been found.

1.4 Objectives

The overall objective of the thesis is to provide a safer design which avoids block failure in practice by considering the uncertainties involved. This can be broken down into two objectives. The first is to quantify the model uncertainty of today's design tools and study possibilities to improve them. The second is to study the applicability of partial factors in the design of block stability in tunnels.

The first objective, regarding model uncertainty, involves different issues such as describing the model uncertainties of kinematic limit equilibrium (KLE) analysis and today's analytical models, improving the understanding of the failure mechanism involved and proposing a new analytical solution.

1.5 Limitations

Although block failure is a three-dimensional problem, a two-dimensional modelling approach was developed. In general, a two-dimensional approach is more conservative than design based on a three-dimensional model according to Duncan (1992) and Stark and Eid (1998). A two-dimensional model assumes the maximum possible block along the entire tunnel length, while in a three-dimensional model, discontinuities cross each other and form smaller blocks.

For the mechanical model, a symmetric block was considered. The in-situ stresses were taken into account, with the vertical and horizontal stresses being the principal stresses. The joint friction angle was considered to be independent of normal stress. The joint friction angle is increased by decreasing normal stress (Jing, 1992). However, in most of the cases studied by Jing, the influence of normal stress on the joint friction angle is not

significant. Block movement gives unloading of the block (Bagheri, 2009); therefore a lower friction angle, which will ignore the dependence of the normal stresses on the joint plane, results in a safer design.

Model uncertainty can only be quantified through comparison either with other more detailed models that exhibit a closer representation of nature or with data collected from the field or the laboratory (Ditlevsen, 1982). The author has not found cases recorded in which failed block geometry, volume, resistance parameters and stresses were measured. Therefore, the results of KLE and analytical solutions have been compared to those that are more closely representative of nature, like numerical methods such as the DEM and DFN-DEM approaches.

1.6 Structure of the thesis

The thesis has two parts. The first part of the thesis (Chapters 2 and 3) considers the model uncertainty of kinematic limit equilibrium (KLE) and analytical solutions. The second part (Chapter 4) includes a sensitivity analysis and the application of partial factors to design against block failure.

Chapter 2 discusses conventional design tools based on KLE to estimate block stability. Different methods for estimating block volume are available. Kinematic analysis and discrete fracture networks are two common ways to estimate block volume. Kinematic analysis can be used in different manners with both limited and unlimited joint length. Kinematic analysis is used in combination with limit equilibrium to analyse forces. Discrete fracture networks (DFN) are used together with discrete numerical models (DEM) to estimate both block volume and stability. These two approaches are compared.

An investigation of the mechanical models that consider the stresses acting on a block is performed in Chapter 3. Among the analytical models that consider clamping forces, the Crawford-Bray model is a fundamental solution, and its model uncertainty is estimated. The reason for the model uncertainty of Crawford-Bray is recognised. The failure mechanism with the use of a force polygon is extended, and a new analytical solution that considers more realistic clamping forces for block stability is proposed. The solution is verified by comparing it to DEM, and the model uncertainty of the new solution can be determined.

The new analytical solution is applied to ultimate limit state design to assess sensitivity factors and, critical sensitivity factors are proposed in Chapter 4. Based on them, partial factor is calculated and rock support designed using the partial factor method is compared to rock support designed by FORM. A discussion of the results of the study and outcome of the research is provided in Chapter 5. Suggestions for further research on block stability analysis are presented in Chapter 5.

Chapter 2 is the result of the first journal article, “Design Consideration of Large Caverns by Using Advanced Drilling Equipment” together with the conference paper “Some Aspects of Model Uncertainty in the Calculation of Block Stability Using Kinematic Limit Equilibrium”. Chapter 3 pertains to the second and third journal articles, “Investigation of Model Uncertainty for Block Stability Analysis” and “A New Analytical Solution Based on Joint Relaxation for Analysing Symmetrical Block Stability”, while Chapter 4 concerns the fourth journal article, “Application of Partial Factors to Block Stability Analysis”. These five papers are presented as appendices to the thesis.

Chapter 2 Review and discussion of today's design tools

2.1 Introduction

This chapter is based on the first journal article together with the conference paper and parts of my licentiate thesis. The main objective is to compare different design tools and study the accuracy of them in analysing block stability.

2.2 Block stability

The first question that must be answered in analysing block stability is ***What are the shape and size of the block?*** There are different design tools for estimating block volume such as image processing (Kemeny et al., 1993), Discrete Fracture Network (DFN) modelling (Dershowitz and Einstein, 1988), stereological methods such as kinematic analysis (Dinis, 1977; Kleine, 1988; Villaescusa and Brown, 1991) and experimental equations based on RQD (Palmstorm, 2005).

Two common methods for estimating block volume are kinematic analysis and DFN. The main difference between DFN and kinematic analysis is that kinematic analysis takes into account blocks formed by the conjunction of three joint sets, while in DFN, blocks can be formed by the conjunction of more than three joint sets. In other words, in kinematic analysis, blocks are assumed to have a tetrahedral shape while other polyhedral shapes of blocks are possible with DFN modelling. Another difference is that the aim of kinematic analysis is to find the maximum block possible while this is not

the case with DFN. Different design tools based on different assumptions may result in different results, and the designer must be aware of this.

The second question is *Is the block stable?* The question involves quantifying the forces and analysing the equilibrium of the block. In excavating, the state of stress changes, so the forces acting on the block change as well. This may influence the stability of the block. Design tools to address this second question are divided into two groups, analytical methods and numerical methods. Analytical design tools are categorised into two sub-groups. One is based on limit equilibrium and the other considers relaxation due to joint deformation. Table 2-1 shows various combinations of different design tools to address the question of block volume and analyse forces that act upon the block equilibrium.

Table 2-1. Different design tools for analysing the geometry and stability of blocks (Bagheri, 2009)

<div><div><i>Block volume estimation</i></div><div><i>Equilibrium estimation</i></div></div>			<i>Kinematic analysis</i>			<i>DFN</i>
			Unlimited joint length	Finite joint length		
				Deterministic	Probabilistic	
Analytical methods	Limit equilibrium methods	No stress field (1)	A1	B1	C1	D1
		Considering stress field (2)	A2	B2	C2	D2
	Joint relaxation is considered (3)		A3	B3	C3	D3
Numerical discrete methods	DEM (4)		A4	B4	C4	D4

In the table, the letters A-D refer to the design tools used to estimate the block's existence and volume. The numbers 1-4 refer to the design tools used to analyse forces around a block. A1, B1, B2, are the most common design tools and will be studied further in this chapter. D4 is the most advanced method and may be considered closest to reality. The analytical method based on joint relaxation, 3, will be discussed in Chapter 3.

Conventional kinematic limit equilibrium refers to the case in which the joint length is unlimited and the stresses do not act on the block (A1 in Table 2-1). The effects of joint length on block volume estimation have been discussed in Villaescusa and Brown (1991) and Kim et al., (2007). The limited joint length KLE method considers the maximum joint length observed for the formation of the block, but without any stress acting on the block (B1). In the third KLE method, the joint length is limited to the maximum value observed, and the stress effect is considered by approaching the theories of limit equilibrium (B2).

There is always variation in the joint geometric data, and it is very hard to find a representative value for them. The deterministic approach will result in a block volume that cannot show the influences of input data variation. Therefore, the application of probabilistic methods in joint geometric analysis is inevitable. Kinematic analysis is performed in the probabilistic approach, with input data such as joint length and orientation considered stochastic values and the deterministic values of stress field applied (C2). A Monte Carlo simulation could be used for this purpose.

The DFN modelling is based on stochastic representations of joint systems using the probabilistic density functions of joint parameters (orientation,

size and location in 3D modelling) that are formulated based on field mapping results.

In order to evaluate the block volume around an excavation using the DFN approach, a large number of DFN realisations should be generated. Moreover, there is no criterion for determining how many realisations are required to analyse block stability (Hadjigeorgiou, 2005). It is very important to use appropriate numbers of DFN realisations for numerical modelling, which is still an issue debated among researchers in this field.

The fracture networks generated can be imported into DEM in order to analyse the equilibrium of the blocks. The DEM is an explicit discrete element method based on finite difference principles, which originated in the 1970s with the landmark work on the progressive movements of rock masses as rigid assemblages (Cundall, 1971). The DFN-DEM, D4, approach could be used for block stability analysis.

2.3 Application of today's design tools (a case study)

2.3.1 Introduction

In order to describe the difference between the various KLE methods, the most common design tools used today, a case study in south-eastern Sweden is analysed. A DFN-DEM analysis is carried out to describe reality. The influence of joint length and stress on the design as well as the accuracy of these design tools are discussed in the study, which illustrates the shortcomings of the design tools used.

2.3.2 KLE approach

Different deterministic approaches of KLE, with both unlimited and limited joint length, were combined with different deterministic approaches of limit equilibrium, which both consider and ignore stresses, and were applied to a case to study the accuracy of KLE. A probabilistic approach of KLE (PKLE) was also applied. A code based on FORTRAN was developed to select the values for joint length and joint orientation. In this approach, the input data for estimating block volume (including joint orientation and joint length) were based on a probabilistic approach. The stress field to analyse the equilibrium was based on deterministic values. UNWEDGE software, which is based on KLE, was used to perform the analyses to estimate the volume of unstable blocks per 1 m of tunnel length (based on PKLE). The results of different deterministic and probabilistic approaches of KLE were compared to results from a DFN-DEM analysis, which was calibrated to field observations, Fig. 2-1.

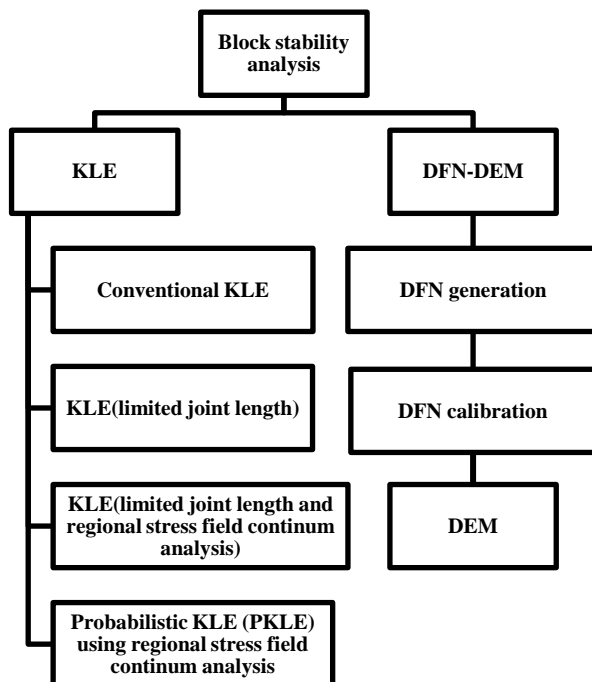


Fig. 2-1. Methods for estimating block stability in the case studied

2.3.3 DFN calibration

In this study, the Watson-Williams (W-W) statistical test was used to find the most similar DFN realisations with a mapped joint pattern from the field. The W-W test is a statistical test of means for spherical data, which is conducted on the composite data set to determine the equivalency on the mean joint orientations from two sets of observations. In this method, the joint orientation measurements are converted to polar coordinates for the calculation of a resultant vector. The length of the resultant vector is a measure of the concentration around a mean direction, if one exists. The calculated resultant lengths are used in a statistical F-approximation to test whether or not the mean joint orientations of the two data sets are

statistically different. The null hypothesis for the F-test states that the mean directions from two samples are not significantly different. This hypothesis is rejected when the F statistic calculated is greater than the critical value for a desired level of significance (Mardia, 1972; Batschelet, 1981).

The joints in the roof and walls of the cavern and a cross-cut perpendicular to it were mapped (Berglund, 2001). The W-W test was applied to both mapped tunnel surfaces (a cross-cut of the cavern and the main cavern). First, 100 DFN realisations were generated. A code in FORTRAN was developed based on the W-W test to check the compatibility of DFN realisations with the results of joint mapping. Out of 100 DFN realisations, 9 were good matches with both (the main cavern and cross-cut tunnel) joint mapping surfaces in the field.

Fig. 2-2 shows schematically the exposed area of a block in the roof of the cavern. The exposed area from joint mapping has a mean value of 2.69 m^2 . Using the DFN calibrated approach, the mean value for the exposed area was calculated as 2.7 m^2 . The similarity between the exposed area from joint mapping and DFN confirms the validity of the DFN calibration using the W-W test.



Fig. 2-2. Exposed area of a block in the roof

2.3.4 DFN-DEM approach

The block assemblages, confirmed by the W-W statistical test, were analysed using DEM in 2D. Fig. 2-3 shows a pattern of the failed blocks from a DFN-DEM analysis. The red vectors show the displacements, and the assemblage of blocks is represented in green. The estimated failed blocks in this analysis include both secondary blocks and other blocks located in the perimeter of the cavern. Secondary blocks are blocks that do not share a cavern boundary. The purpose is to distinguish the key blocks from other types of failed blocks in the block assembly. In order to distinguish between different block types, reference must be made to different block types proposed by Goodman and Shi (1985). Fig. 2-4 shows an enlarged section marked by a blue line inside Fig. 2-3. As can be seen in Fig. 2-4, block number 1 can definitely be categorised as a tapered block and block number 2 as a key block.

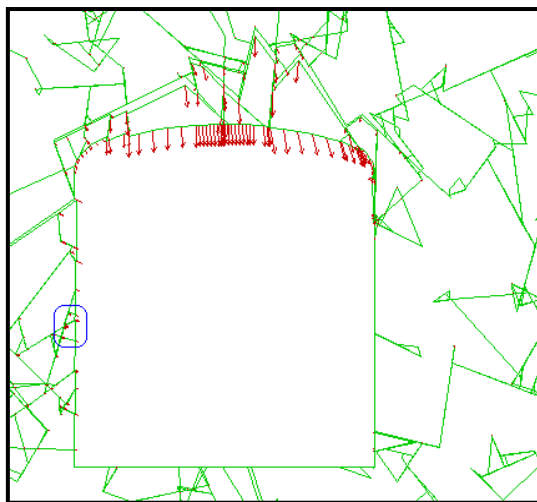


Fig. 2-3. Failed block around the cavern

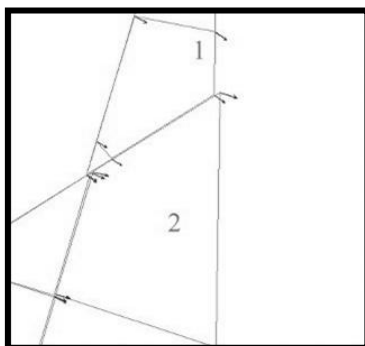


Fig. 2-4. Key block and tapered block around the cavern

The length of the joint in the third dimension of the block was calculated as the square root of the block area. This implies that the joint in the third dimension has a length proportional to the length of other joints. Based on the third dimension of the block, it is possible to calculate the block volume for 1 m of tunnel length. The number of blocks per 1 m of tunnel length can

also be obtained by determining the third dimension. For instance, when the block area is 0.25 m^2 , the third dimension of the block is $l = \sqrt{0.25} = 0.5 \text{ m}$, so the block volume is $V = 0.5 \times 0.25 = 0.125 \text{ m}^3$. Therefore, in each unit length of tunnel, there may be two blocks with this volume.

2.3.5 Results of applying design tools

Unstable key block volumes from the different approaches (A1, B1, B2, C2 and D4) for 1 m of tunnel length are presented in Table 2-2.

Table 2-2. Estimated volume of unstable key block for different design tools for 1 m of tunnel length.

Kinematic limit equilibrium analysis (m^3/m of tunnel length)				DFN-DEM (m^3/m of tunnel length)
Conventional	Limited joint length	Limited joint length and regional stress field	Probabilistic Kinematic limit equilibrium Regional stress	Regional stress field
5778	30.4	21.8	0.05	0.34

The possible unstable block volume was calculated for different combinations of joint sets using KLE approaches. The first approach, ignoring stress field and joint length limitation, results in an enormous amount of block volume that must be supported. The maximum joint length observed in the field was 25m (Starzec, 2002); applying the joint length, the unstable block volume is $30.4 \text{ m}^3/\text{m}$ of tunnel length. The horizontal stress was set at 6.6 MPa, which was measured in a CLAB2 cavern and has an overburden of 30 m (Fredriksson et al., 2001). By applying the regional stress field, some of the unstable blocks become

stable due to the clamping forces. Fig. 2-5 shows the distribution of unstable key block volume for 1 m length of tunnel resulting from PKLE.

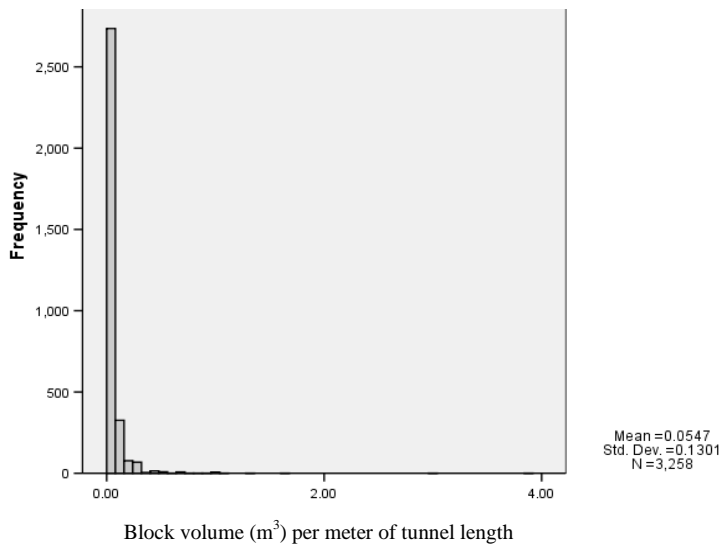


Fig. 2-5. Key block distribution resulting from PKLE

Fig. 2-6 shows the unstable key block volume distribution resulting from DFN-DEM for the unit of tunnel length.

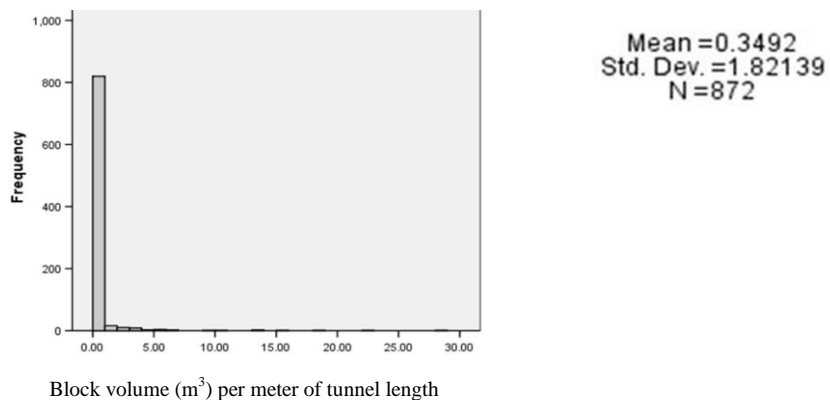


Fig. 2-6. Distribution of key block volume resulting from DFN-DEM

2.4 Discussion

By comparing the exposed area of field mapping with DFN realisations and applying the Watson- Williams test, a basis for a DFN-DEM analysis was established which was used to describe the actual case.

The conventional KLE approach, which does not consider the joint length and field stresses, results in an enormous volume of unstable block. By considering the joint length in KLE, the estimated unstable block volume is reduced. Still, this approach is far from reality. Considering stress field together with joint length will further reduce the unstable block volume. However, this approach is on the safe side and entails overdesign. It can also be concluded that a kinematic analysis based on a Monte Carlo simulation estimates a block volume that is smaller than in reality.

None of the KLE approaches provides results close to DFN-DEM, which was closer to reality, and there is a significant difference between them. The calculated volumes of possible failed blocks using the PKLE method yield results that are almost six times smaller than those from a DFN-DEM analysis.

The reason for this significant difference could be that, in a DFN-DEM analysis, joint termination is taken into account while, in a KLE analysis, it is not. The joint termination ratio is defined in ISRM (1978) using the following formula:

$$T_i = \frac{100N_i}{N_i + N_a + N_o} \quad 2-1$$

Where N_i , N_a and N_o are, respectively, the total number of discontinuities whose semi-trace terminations are in intact rock, are at other discontinuities

or are obscured. These have been calculated for a complete scan line sample or for a specific discontinuity set. A larger value for the joint termination ratio indicates that a large portion of discontinuities terminates in the intact rock. Therefore, in a rock mass such as this, a large number of rock bridges are created compared with the expected discrete blocks, which means that the size of the blocks generated is much larger than the case in which the joint termination ratio is small. Starzec and Anderson (2002) reported the ratio to be around 13% of the joints terminating in intact rock in that case study, while the KLE analysis neglects this ratio.

Fig. 2-7 shows the joint system before eliminating the incomplete joints in UDEC (a numerical code based on discrete element theories). In this program, dead-end joints (terminated joints in intact rock) are eliminated, as shown in Fig. 2-4. Elimination of incomplete joints decreases joint intensity; consequently, estimated block volumes are increased. DEM considers the joint relaxation while limit equilibrium does not consider this. Therefore there are joints that slip and fail due to relaxation but do not slip and fail in the limit equilibrium method.

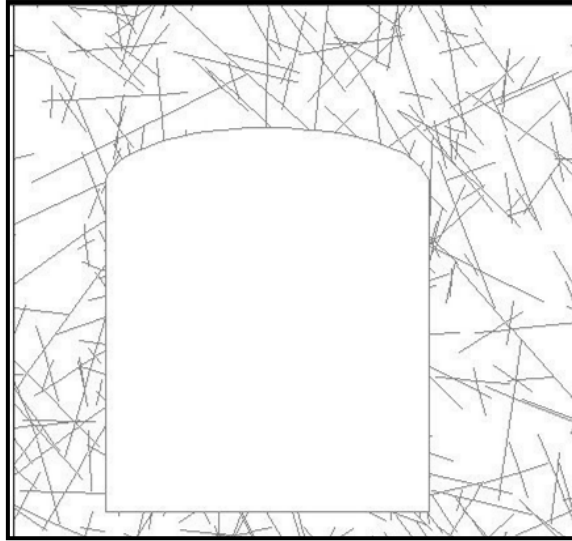


Fig. 2-7. Joint network before eliminating incomplete joints

2.5 Summary and conclusion

The results show that, even considering limited joint length in a kinematic analysis and the clamping forces in the limit equilibrium analysis, there seems to be great model uncertainty in our standard design tools for block stability analysis. It confirms what many researchers, including Goodman and Shi (1982), Curran et al., (2004), Elsworth (1986) and Diedrichs (2000), have noted: that ignoring stress field produces an uneconomical design.

The probabilistic approach analyses (both PKLE and DFN-DEM) give a distribution of the potential unstable block volume. This will show the designer the probability of forming a block with a specific volume. The designer can then decide on the acceptable unstable block volume in terms of its probability.

The volume of unstable blocks with probabilistic kinematic limit equilibrium is lower than DFN-DEM because of the incomplete solution of

limit equilibrium, while DEM considers a complete solution including in-situ stress, excavation and the influence of gravity. However, calculations based on DFN-DEM take a lot of time for generating joints, solving the model and interpreting the results.

Conventional KLE does not provide an economical design. Joint length plays a significant role in determining block volume in a kinematic analysis. Confining stresses play an important role in the stability analysis of a block. The information about joint length and stresses could lead to a better design. The costs of obtaining the information about the joint length and stresses must be compared with the costs of overdesign.

Model uncertainty exists because of unrealistic assumptions in the block volume estimation and incorrect estimation of clamping forces. Clamping forces are estimated incorrectly because of an incomplete understanding of the failure mechanism. In the following chapter, the failure mechanism will be studied further in order to identify an accurate solution.

Chapter 3 Analytical methods based on joint relaxation

3.1 Introduction and history

Analyses in Chapter 2 show that the stress field, which provides confining stresses around the block, could significantly increase the stability. Therefore a correct estimation of clamping forces is a critical issue in analysing block stability. The analytical method proposed by Crawford and Bray (1983) assumes that the clamping forces before excavation will not change during or after excavation. Works such as Elsworth (1986), Sofianos (1986, 1999) and Nomikos (2002, 2006) attempted to address this and use the redistributed stresses to estimate clamping forces. However, block failure is still observed, and the estimated clamping forces are questionable. The objectives of this chapter are to estimate the model uncertainties for the Crawford-Bray solution and propose a new solution to calculate the clamping forces that considers the relaxation and redistribution of the stresses. This chapter is mainly the outcome of journal articles II and III, which discuss how to estimate the clamping forces for analysing block stability.

3.2 Crawford-Bray solution

Crawford and Bray (1983) proposed the following equations (3-1 and 3-2) to calculate the ultimate pull-out force, T , and displacement, δ :

$$T = \frac{2H(K_s \cos^2 \theta + K_N \sin^2 \theta)(\tan \phi - \tan \theta)}{(K_s + K_N \tan \phi \tan \theta)} \quad 3-1$$

$$\delta = \frac{H(\tan \varphi - \tan \theta)}{(K_S + K_N \tan \varphi \tan \theta)} \quad 3-2$$

Where H is the clamping forces, θ is the half-apical angle of the triangular block, φ is the joint friction angle and K is the joint stiffness. Subscripts N and S refer to the normal and shear directions.

As was noted by Crawford and Bray (1983), the clamping forces, H , are products of the horizontal in-situ stress prior to the excavation, σ_h , and block height, h .

Below, the initial clamping forces prior the excavation, called the initial clamping forces, are described using three numerical models, which serve as a basis for assessing the model uncertainty of the Crawford-Bray equation, 3-1.

3.3 Initial clamping forces

A study based on numerical modelling has been carried out in order to investigate how the stress field and joint stiffness influence the initial clamping forces.

Three different models, two with a single block in regional and local stress models and one with a block assembly in a local stress model, have been studied using UDEC. The first model assumes that the regional stresses act the same in all points of the model. The local stress model is based on the assumption that the regional stress field acting on the boundaries of the model and the local stresses acting on the block will be the result of deviation due to the relative stiffness of the joints and rock mass. The third model has the same assumptions as the second model but describes a

geometry that includes a block assembly and not a single block. All models will give the same average stresses equal to the regional stress field.

Fig. 3-1, 3-2 and 3-3 illustrate the principal stress distribution before excavating the tunnel for those models (for a case in which $K_S=9.19$ MPa/m and $K_N=45.95$ MPa/m). In the first, the stresses are distributed equally throughout the model from the regional stress model, Fig. 3-1; therefore the initial clamping forces are independent of joint stiffness and are equal to that proposed by the Crawford-Bray equation ($H=\sigma_h \times h$).

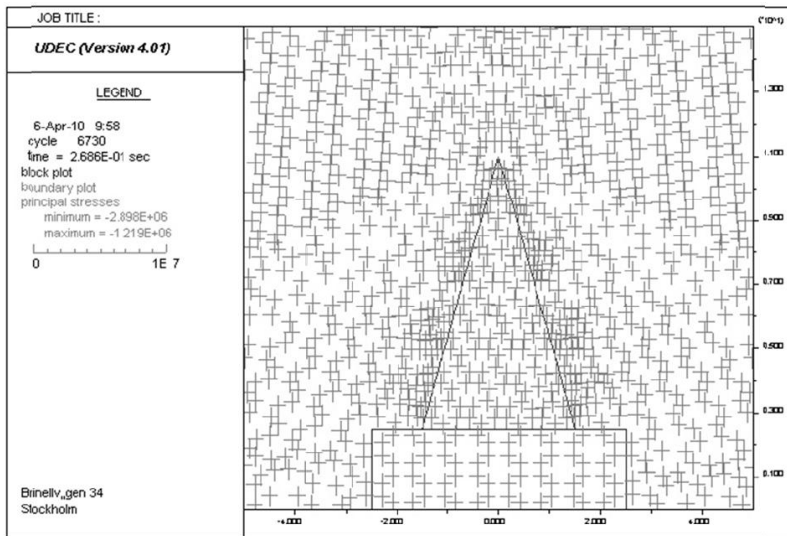


Fig. 3-1. Regional stress model (first model)

The pattern of stress distribution in the local stress model depends on the joint stiffness, and stresses pass around the weaker joints. This indicates that the initial clamping forces are lower for joints with lower joint stiffness. Fig. 3-2 shows that the major principal stresses are parallel to the joint plane and no forces are transmitted across joints if the stiffness is low enough. The

stresses in the block are significantly smaller than stresses around the block, which is seen as a blank space in the figure.

The joint friction angle has been mobilised so that it is equal to the arctangent of the ratio of shear force to normal force. The mobilisation of the joint friction angle is increased by decreasing the joint stiffness.

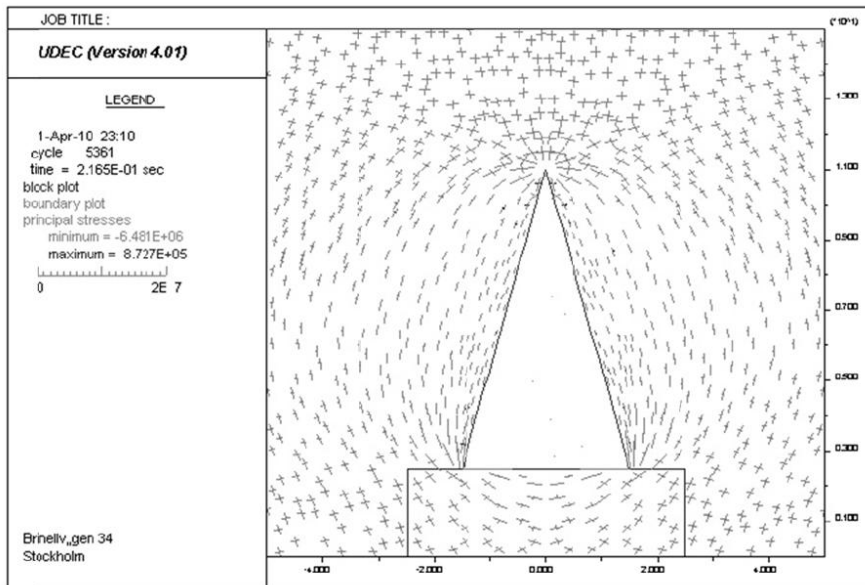


Fig. 3-2. Local stress model (second model)

Models with a block assembly, Fig. 3-3, were run for the local stress model to understand the influence of the block assembly on the initial clamping forces. It was observed that the initial clamping forces are equal to the regional stress model.

To summarise, local stresses determine the initial clamping forces on the block. In the local stress model, with lower joint stiffness, the friction angle is more mobilised and the clamping forces are lower. A single block has

lower clamping forces compared to a block assembly and thus will give a design on the safe side. Below, an assessment of model uncertainty based on the methods noted above was performed.

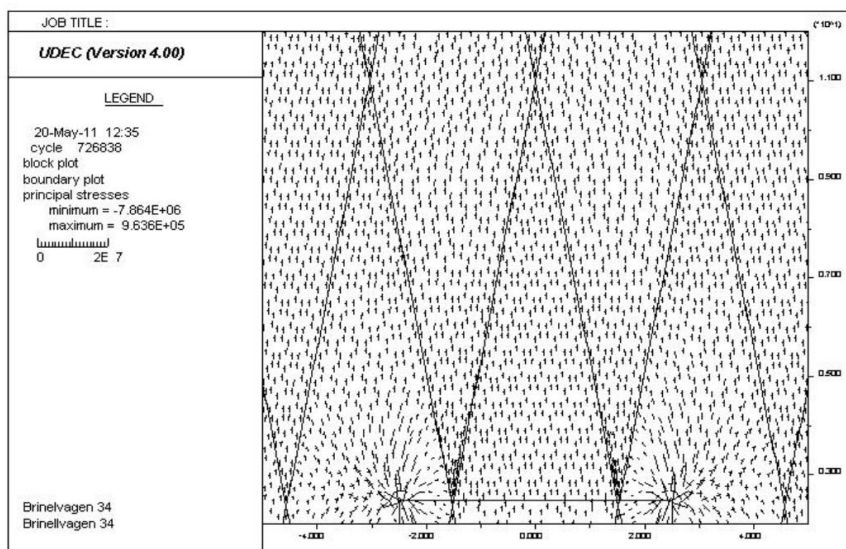


Fig. 3-3. Local stress model assemblies (third model)

3.4 Model uncertainty of the Crawford-Bray solution

3.4.1 Methodology to assess model uncertainty

Model uncertainty is quantified by a comparison with other, more detailed models that more closely represent nature or with data collected from the field or laboratory (Ditlevsen, 1982). There is a lack of cases recorded for a failed block in which geometry, volume, resistance parameters, and stresses were measured. Therefore, the results of the Crawford-Bray model were compared to the results of the Discrete Element Method (DEM), which more closely represents reality. An assessment of the model uncertainty, I, was performed using the ratio of the ultimate pull-out force calculated using

DEM, T_{Numeric} to the ultimate pull-out force based on the analytical solution (Eq. 3-1) $T_{\text{Analytic}}, I = \frac{T_{\text{Numeric}}}{T_{\text{Analytic}}}$ for the same loading geometry and properties conditions.

The deformable body was chosen for an analysis in UDEC. The model uncertainty of the analytical solution was estimated for different depths, stresses, resistance properties and block geometries (half-apical angles). Cases in which the half-apical angle is equal to or greater than the friction angle were ignored. The values of joint shear stiffness could be calculated based on Eq. 3-3 (Barton and Choubey, 1977).

$$k_s = \frac{100}{L} \sigma_n \tan \varphi \quad 3-3$$

The input data in Eq. 3-3 are the normal stress acting on the joint plane, σ_n , total joint friction (φ), and joint length (L). With values known for the vertical and horizontal stresses, the value of σ_n could be calculated from a continuum analysis, such as BEM, on the joint plane. For different conditions of in-situ stress and the half-apical angle, the calculated σ_n varied between 0.11 and 23.47MPa. Three different stiffness ratios were considered for each σ_n (Bagheri, 2009). Joint length was calculated for a geometry in which the block has the specific half-apical angle and a base of 3 m.

Joint normal stiffness was chosen based on the joint shear stiffness and the stiffness ratio, $R = K_N/K_S$, of the joint, which depends on the normal stress (Bandis et al., 1983). As shown in Fig. 3-4, there are different ratios of normal to shear stiffness depending on the normal stress (for example, for $\sigma_n = 0.2$, the possible range is between 10 and 40; 10, 20 and 40 were chosen). Beyond 0.5MPa, the ratio decreases with an increasing σ_n towards an

asymptotic value of approximately 10. It seems reasonable to assume that the ratio is within the range of 1 to 10 if the normal stress, σ_n , is larger than at least 0.5MPa (Oda et al., 1993). In both the numerical and analytical models it was assumed that the joint stiffnesses are constant and do not change with changes in normal stress.

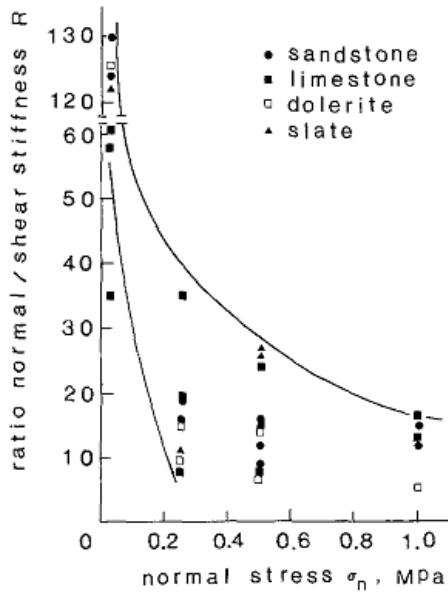


Fig. 3-4. Dependence of stiffness ratio (R) on normal stress (Bandis et al., 1983)

3.4.2 Results of simulations

Fig. 3-5 shows the results of simulations based on the regional stress model. A total of 243 models were built at different depths (20-400 m), half-apical angles (10^0 - 40^0), friction angles (30^0 - 50^0), and horizontal and vertical stresses (K_0 varies between 0.5 and 2).

The negative sign indicates that the analytical solution predicts the block is stable while DEM predicts the block is falling. The range is between -1 and 1. The mean value for the model uncertainty factor is 0.42.

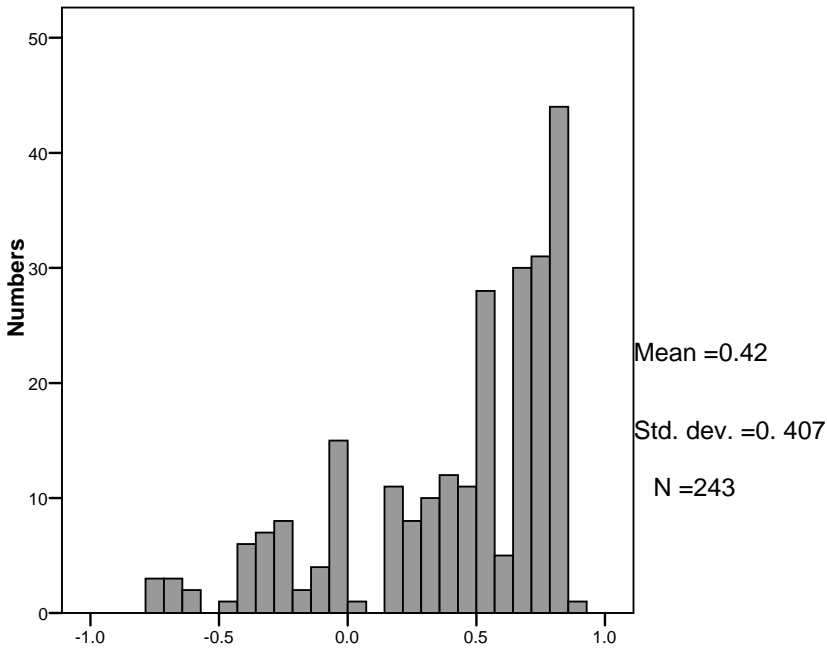


Fig. 3-5. Model uncertainty of the Crawford-Bray solution (numerical model based on regional stress)

The model uncertainty was also calculated for cases of a half-apical angle equal to 10 degrees and different depths (20, 100 and 400 m), $K_0(0.5, 1$ and $2)$, and a friction angle (30° - 50°) based on the local stress model with a single block. The results are presented in Fig. 3-6.

The uncertainty of the Crawford-Bray model assuming a local stress field is more than that calculated using the regional stress model. This is because of the mobilisation of the joint friction angle with soft joints in the local stress model before excavation. No mobilisation of the soft joints in the regional stress model was observed.

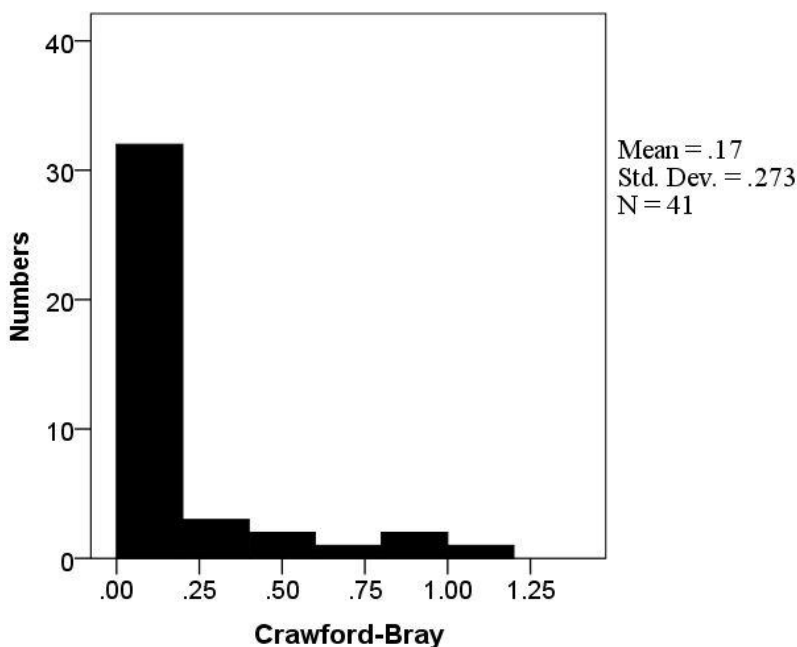


Fig. 3-6. Model uncertainty of the Crawford-Bray solution (numerical model based on local stress)

3.4.3 Reasons for model uncertainty

The analyses show a significant difference between the results of DEM and the analytical solution (see Fig. 3-5 and 3-6). The cases selected for a detailed discussion are for a depth of 100 m and $K_0=0.5$ with different stiffness ratios, R (1, 5 and 10). The unit weight was considered as $2,700 \text{ kg/m}^3$. The clamping forces calculated based on continuum mechanics by BEM are 11.9 MN. The input data are described in Table 3-1.

Table 3-1. Input data for the block analysed

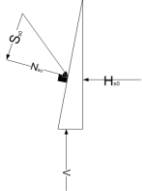
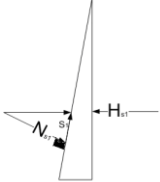
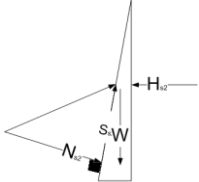
Parameter	Value
Half-apical angle (degree)	10
Friction angle (degree)	30
Joint shear stiffness (MPa/m)	9.19
Vertical stress (MPa)	2.5
Horizontal stress(MPa)	1.25
Joint length (m)	8.6

Table 3-2 shows displacement and forces (normal, shear and clamping) at different stages of relaxation from the numerical regional stress model. The stress state changes when the tunnel is excavated. The gravity force does not act at this stage. This stage could be called the first stage of relaxation (after excavation and before the acting gravity force). The numerical solution shows a considerable amount of shear displacement in the joints in this stage. As is shown in Table 3-2, the normal force in this stage is reduced, and the sign of the shear force changes. The changes in the sign of the shear force mean that the direction of the shear force changed due to relaxation of the in-situ stress.

The analytical solution proposed by Bray and Crawford does not calculate the relaxation of induced stress. The amount of relaxation in this stage is much higher compared to the final stage, the last column in Table 3-2.

Relaxation produces a lower normal force. Reducing the normal force acting on the joint means having lower safety, and the block is closer to failure. This is why the DEM predicts lower safety for blocks.

Table 3-2. Force and displacement in different stages of relaxation from numerical solution (regional stress model)

K_N/K_S	Parameter			
		In-situ forces before the excavation	Forces state after the excavation without acting gravity force	Forces state after acting gravity force
R=1	N(MN)	11.1	10.5	10.4
	S(MN)	-1.84	1.85	2.01
	H(MN)	10.61	10.66	10.59
	δ (mm)	0	47.64	49.77
R=5	N(MN)	11.1	8.24	8.12
	S(MN)	-1.84	1.45	1.6
	H(MN)	10.61	8.36	8.27
	δ (mm)	0	42.56	44.45
R=10	N(MN)	11.1	6.06	5.85
	S(MN)	-1.84	1.07	1.2
	H(MN)	10.61	6.15	5.96
	δ (mm)	0	37.6	39.22

3.4.4 Summary and conclusions of the Crawford-Bray solution

DEM considers the relaxation of induced stress, while the Crawford-Bray solution does not. The relaxation of in-situ stress gives joint normal displacement, which reduces the clamping forces. This is not considered in the analytical solution; therefore, the analytical solution may overestimate block stability.

The ultimate pull-out force in the analytical solution (T_{analytic}) depends on four parameters (the apical angle, the friction angle, horizontal in-situ stress and the ratio between joint normal and shear stiffness). The DEM solution considers six parameters as input data (vertical and horizontal in-situ stress, shear and normal joint stiffness, the apical angle and the friction angle). DEM requires not only the ratio between shear and normal joint stiffness but also values of shear and normal joint stiffness and vertical in-situ stress. Ignoring key parameters such as joint shear and normal stiffness together with the first stage of relaxation leads to uncertainty in the model. The reason for model uncertainty was thus identified, and further studies will be carried out in order to propose a new solution to quantify joint relaxation and calculate the clamping forces on the block.

3.5 *New conceptual model*

In order to understand how the clamping forces change in relation to loading and unloading, a conceptual model of block behaviour was developed based on four stages. The conceptual model and the development of clamping forces are illustrated schematically in Fig. 3-7. In reality, however, all the stages occur quickly and simultaneously, but for ease of understanding, the problem was divided into these four stages.

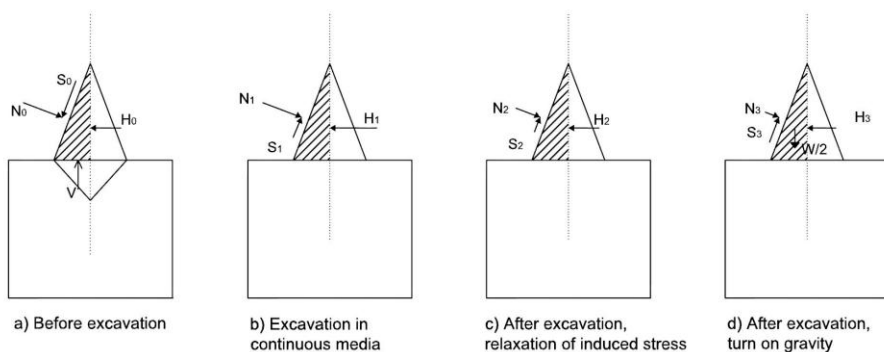


Fig. 3-7. Conceptual model of block behaviour

Fig. 3-8 shows the corresponding force polygon for the different stages based on the conceptual model and illustrates in particular how the clamping forces change from one stage to another. Since the block is assumed to have symmetric geometry, only half of it was considered. N and S denote the normal and shear forces acting on the joint defining the block while H , W and V denote the clamping forces, the weight of the block and the initial vertical load acting on the half-block. The index is connected to the different stages, as can be seen in Fig. 3-7 and 3-8. Thick lines in Fig. 3-8 show the Mohr-Coulomb failure criterion. The force polygon must be located within the stable range defined by the failure criterion. This implies that the absolute value of the ratio of shear to normal forces, $\left| \frac{S}{N} \right|$, must be

lower than $\tan \varphi$. As the ratio of $\left| \frac{S}{N} \right|$ gets closer to $\tan \varphi$, the joints get

closer to failure. As mentioned in paper II, the vertical stress, angle ratio and ratio of the half-apical angle to the friction angle are important parameters in estimating model uncertainty. This is shown in Fig. 3-8 A; by increasing vertical stress, the vertical force, V , is increased and the ratio of shear to

normal forces, $\left| \frac{S}{N} \right|$, gets closer to the failure line. Moreover, by increasing the angle ratio, the force polygon gets closer to the failure line. Getting closer to the failure line means more mobilisation of the joint friction angle.

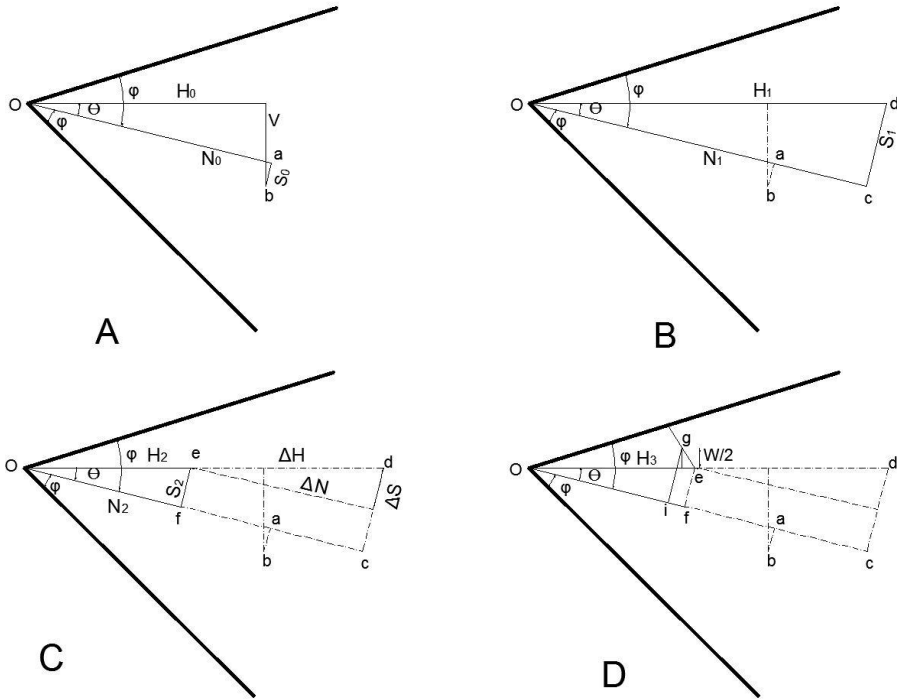


Fig. 3-8. Force polygon diagram of the forces acting on the block after each stage based on the conceptual model given in Fig. 3-7

3.6 New analytical solution

Fig. 3-9 shows the relaxed forces on three components of the system – the block, the joint and the surrounding rock. Based on compatibility and equilibrium conditions for the components of the system, Eq. 3-4 and 3-5

were found to calculate the relaxation of induced forces due to the presence of joints for a symmetric block.

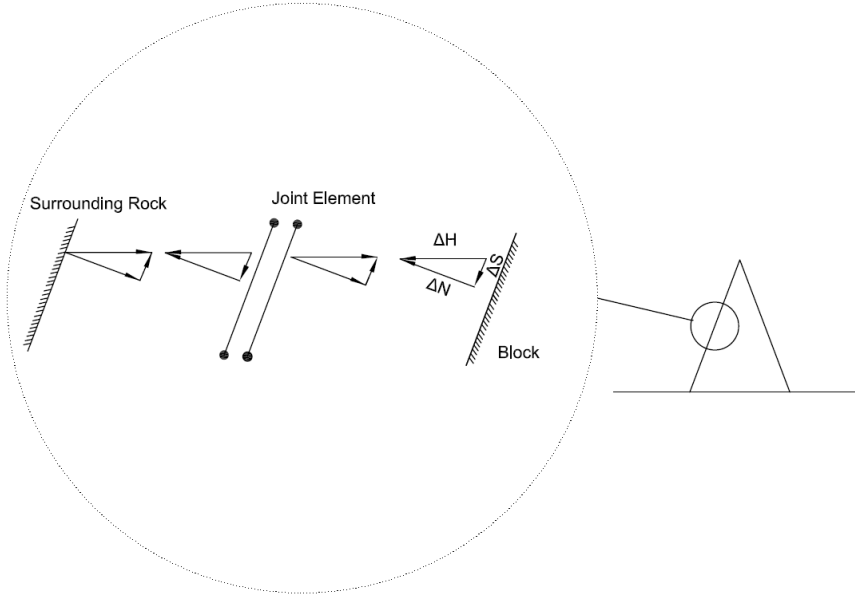


Fig. 3-9. Relaxed forces on the components of the system

$$\Delta N = \frac{\frac{S_1}{K_S} \tan \theta + \frac{N_1}{K_N}}{\tan^2 \theta \left(\frac{1}{K_{S,R}} + \frac{1}{K_S} \right) + \frac{1}{K_{N,R}} + \frac{1}{K_N}} \quad 3-4$$

$$\Delta S = \Delta N \times \tan \theta \quad 3-5$$

There are two equations (Eq. 3-4 and 3-5) and two unknown parameters (ΔN and ΔS). The system of equations could then be solved. The acting forces on the block after relaxation (N_2 and S_2) can then be calculated. After

this, the clamping forces, H_2 , in the third stage (oe in Fig. 3-8 C), can be calculated according to Eq. 3-6.

$$H_2 = \sqrt{N_2^2 + S_2^2} = \sqrt{(N_1 - \Delta N)^2 + (S_1 - \Delta S)^2} \quad 3-6$$

3.7 Verification of clamping forces calculated in a discontinuous medium

Two groups of modelling were performed to check the validity of the solution. The first group considers the tunnel at a depth of 100 m and K_0 equal to 0.5 as well as a wide range of different joint stiffnesses from soft to stiff. The second group of modelling checks the validity of the solution for different depths (20-400 m), in-situ stresses (K_0 varies between 0.5-2), and joint friction angles (30-50 degrees). Both groups correspond to the same 41 cases analysed in Fig. 3-6.

Fig. 3-10 shows a comparison between the clamping forces, H_2 , at the third stage, C, calculated using different methods such as DEM, FEM and the analytical solution for the first group of modelling. In this figure, the value of the clamping forces ($H_2=H_1=1.25 \times 8.5=10.6$ MN) suggested by Crawford and Bray as well as from a continuum analysis (BEM) are shown. The clamping forces calculated from both Crawford-Bray and BEM are constant for different joint stiffnesses. Fig. 3-10 confirms that the values of clamping forces calculated using BEM are higher than those using Crawford-Bray and DEM. Fig. 3-10 shows that the estimation based on BEM, which considers stress redistribution, is valid for joints that have a stiffness higher than 100 GPa/m. In the continuum approach, stress redistribution due to excavation is considered, but the influence of stress relaxation due to joints is not taken

into account. Therefore, the clamping forces from BEM are higher than those calculated using FEM with a joint element and the new analytical solution. Note that there is no redistribution due to any excavation taken into account in the Crawford and Bray suggestion.

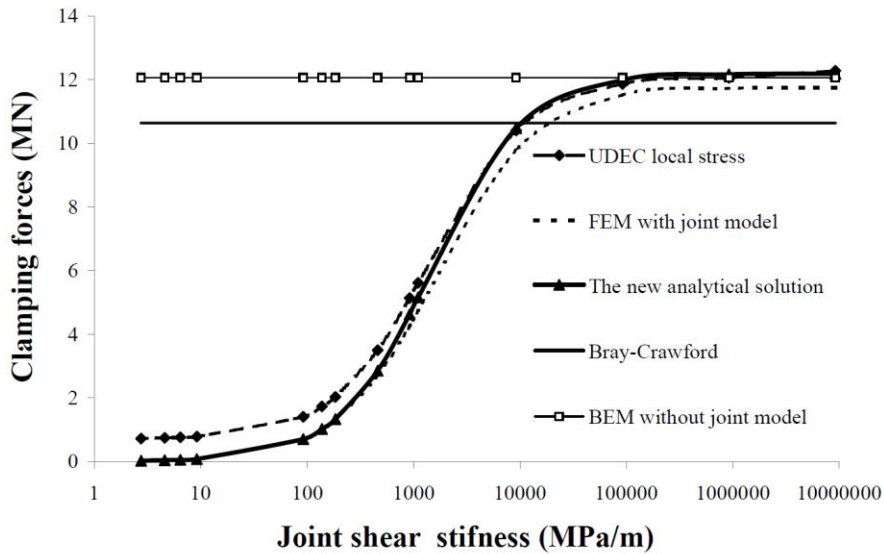


Fig. 3-10. Comparison between the clamping forces at the third stage, C, using different methods

The results from the second group of calculations show a difference between clamping forces from the new analytical solution and the numerical solution; these are shown in Fig. 3-11. The clamping forces estimated by the new analytical solution are a little lower than DEM and are on the safe side, thus satisfying the requirement specified by Eurocode (EN, 1990): “a modification of the results from the model may be used to ensure that design calculation is either accurate or errors on the side of safety”.

Fig. 3-10 also indicates that for the joint with stiffness lower than 1000 MPa/m, the new analytical solution predicts the clamping forces a little lower than DEM.

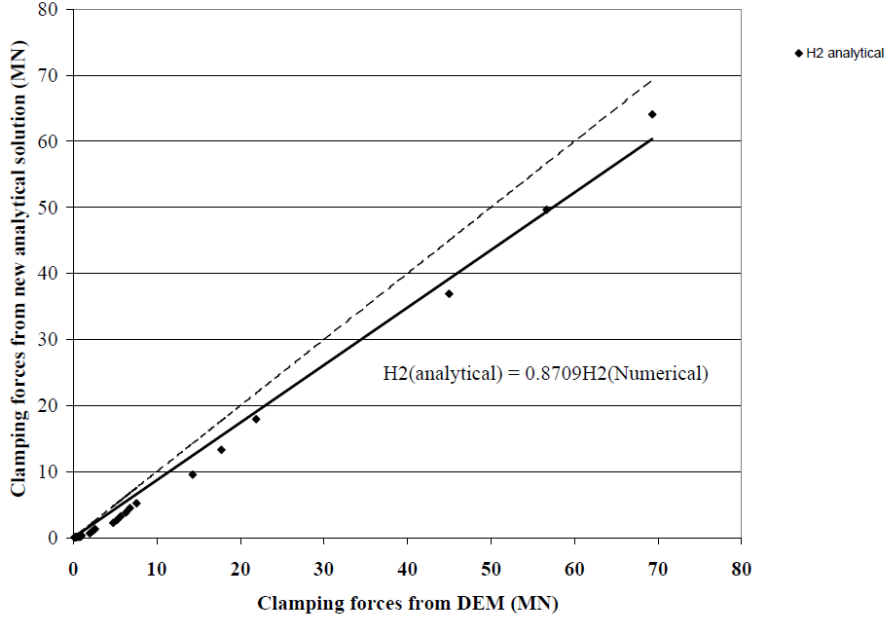


Fig. 3-11. Comparison between clamping forces using different methods for the second group of modelling

3.8 Ultimate pull-out force and model uncertainty calculation using the new solution

The ultimate pull-out force of the block, Stage D, has been calculated using different methods (Crawford-Bray, the new analytical model and the numerical code) for both groups. Fig. 3-6 shows the distribution for the model uncertainty of the Crawford-Bray solution measured for both groups. The mean value of the model uncertainties was 0.17. The cases with a low

value of model uncertainty (those that are biased) correspond to those with a low value of joint stiffness.

The new analytical solution considers joint relaxation and its influence on clamping force reduction while the ultimate pull-out force predicted by the Crawford-Bray solution uses clamping forces independent of joint stiffness. There is good agreement obtained with the new analytical solution, indicating that the new analytical model accurately describes the ultimate pull-out force on the block, Fig. 3-12.

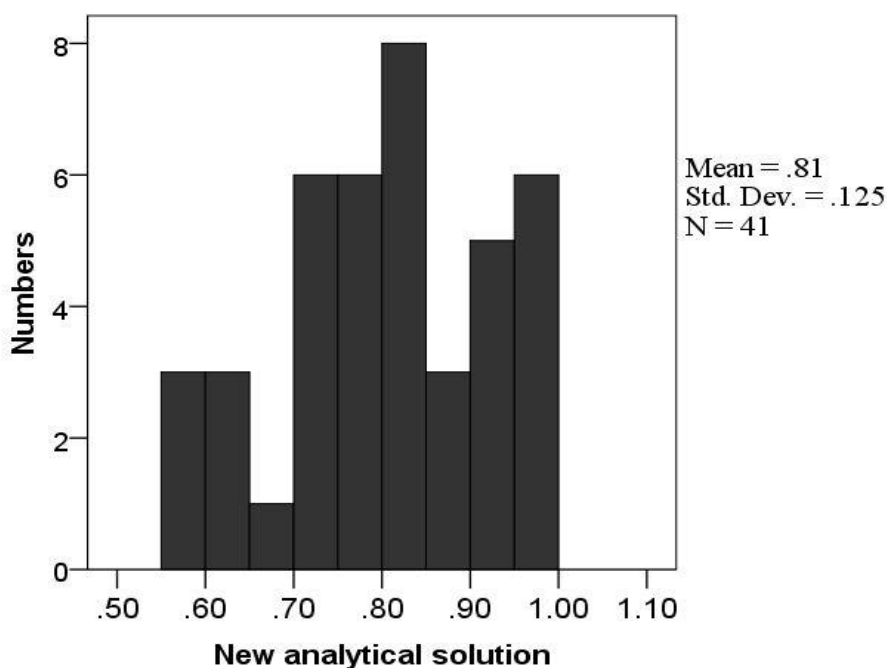


Fig. 3-12. Model uncertainty for the new analytical solution

The mean value of 0.81 indicates that the new analytical solution overestimates the ultimate pull-out force. Even though the clamping forces from the analytical solution are lower than those from DEM, the ultimate

pull-out force from the analytical solution is lower than those from DEM. The reason for that is the new analytical solution ignores the relaxation of the regional stress field due to joint stiffness before excavation. The use of a model uncertainty factor in design counterbalances the overestimation of the ultimate pull-out force.

3.9 Conclusion

Block stability is governed by clamping forces, which is a result of a complex mechanism and interaction between many parameters. The Crawford-Bray analytical solution simplifies the complex mechanism and considers a constant clamping force. The simplification results in model uncertainty. Ignoring model uncertainty for block stability may lead to unsafe and misleading design. An incomplete understanding of the failure mechanism is the main source of model uncertainty in the analytical solution, so a complete understanding of the failure mechanism is crucial.

The complex mechanism has been described by dividing the development of forces acting on the block into stages and using a force polygon. Relaxation of induced stress has a great influence on the amount of clamping forces and is a function of many parameters, such as the stiffness of surrounding rock and joints. The clamping forces from the new analytical solution can be somewhat lower than those from numerical methods.

In addition, relaxation of regional stress before excavation is a key issue in analysing block stability. The initial clamping forces of a single block in a massive rock mass are lower than the clamping forces of a key block with the same size in blocky ground for the same given in-situ stresses.

The proposed analytical solution provides more precise, accurate results that are closer to reality than previous solutions since the mean value and standard deviation of model uncertainty are improved. Numerical modelling can be used to improve the understanding of the failure mechanism and the calibration of analytical solutions.

Chapter 4 Application of partial factors to block stability analysis

4.1 Introduction

The use of a safety factor is traditionally applied to the design of block stability (Bray, 1977; Sofianos et al., 1999). However, the safety factor is not an absolute measure of safety (Honjo, 2009). Use of a partial factor design, which is a type of ultimate limit state design, is recommended by Eurocode (EN 97). Partial factors are proportional to the uncertainties and sensitivity of the parameters. Sensitivity is indicated by sensitivity factors, which are the direction cosines from the origin to the failure surface in a normalised parameter space. The advantage of calculating sensitivity factors is gaining an understanding which input is the most critical and has more influence than others in estimating the probability of failure and will thus require a more precise description. The main objective of this chapter is to study the applicability of partial factors in block stability analysis.

4.2 Methodology and assumptions

The new block stability analytical solution described in Chapter 3, based on the Crawford and Bray solution (1983), was used as the performance function in a reliability analysis. The analysis was carried out using the traditional first order reliability method (FORM). FORM will produce the safety index of the block stability, β , as well as the support needed to achieve a given safety index. The analysis will also produce the sensitivity factors for the different variables.

The partial factors can be validated by a FORM analysis since there is a theoretical link between the partial factors and the safety index and

sensitivity factors. This was done in the study; by carrying out a FORM analysis for different conditions of loads and resistances, the variation in the sensitivity factors for each variable can be assessed. Since the partial factors are considered to be constant for each case (performance function), they are to be evaluated for the most critical combination.

The sensitivity factors for the critical combination have been applied to a number of cases in order to calculate the required rock support based on a partial factor design. For the same cases, FORM was applied to assess the required rock support. The required rock support determined by these two approaches for a given safety index was then compared. This indicates under what conditions the partial factors are applicable.

4.3 Ultimate limit state function

4.3.1 Block stability ultimate limit state function

The ultimate limit state function in its simplest form is formulated in Eq. 4-1, where T is the resistance force and S is the load (block weight).

$$SM = T - S \quad 4-1$$

An estimation of the ultimate pull-out force of the block, T , is subject to model uncertainty. Therefore, the ultimate limit state function is written in the form of Eq. 4-2, where M is the model uncertainty factor. The model uncertainty factor is a random variable that should be considered in the ultimate limit state design. As the mean value approaches 1, the model is closer to reality.

$$SM = MT - S \quad 4-2$$

If the block is supported with rock bolts with a bearing capacity, B, the performance function will be the following:

$$SM = B + MT - S \quad 4-3$$

The resistance force, T, is estimated by modifying the equation proposed by Bray and Crawford (1983), and the load, S, is the block weight. As described in Chapter 3, T is the ultimate pull-out force. Substitution of Eq. 3-1 into Eq. 4-2 gives Eq. 4-4

$$SM = MT - S = M \frac{2 \times H_2 (\cos^2 \theta + R \sin^2 \theta) (\tan \phi - \tan \theta)}{(1 + R \tan \phi \tan \theta)} - V \gamma_w \quad 4-4$$

in which R is the stiffness ratio of the joint (K_N/K_S), θ is the half-apical angle of the block, ϕ is the joint friction angle, γ_w is the rock mass density and V is the block volume. H_2 (clamping forces) is estimated by the formulas Eq. 4-5, 4-6 and 4-7.

$$H_2 = \sqrt{(N_1 - \Delta N)^2 + (S_1 - \Delta S)^2} \quad 4-5$$

$$S_1 = N_1 \tan \theta \quad 4-6$$

$$\Delta S = \Delta N \tan \theta \quad 4-7$$

Substitution of Eq. 4-6 and 4-7 into 4-5 gives Eq. 4-8 for clamping forces.

$$H_2 = \frac{(N_1 - \Delta N)}{\cos \theta} \quad 4-8$$

Chapter 3 introduced Eq. 3-4 and 3-5, which are used to calculate the normal force reduction.

The ultimate limit state function is a complex, nonlinear function. Nonlinearity is not the only complexity of the limit state function; there are also correlations between parameters. These correlations and their mathematical equations are explained in the following section.

4.3.2 Joint stiffness

Joint normal stiffness, K_N , is a function of joint shear stiffness, K_S , and R (the stiffness ratio) (Bandis et al., 1983). Both joint shear stiffness (K_S) and the stiffness ratio are functions of normal stress (Barton and Choubey, 1977; Barton Bandis, 1983). Normal stress on the joint plane is expressed as the ratio between normal force and the joint area (joint length \times 1). Normal force is the normal force from induced stress minus normal force reduction. The normal stresses will change during the relaxation process from N_1 to $(N_1-\Delta N)$. A lower limit of the stiffness can be assessed if the value of the normal stress after relaxation ($N_1-\Delta N$) is used. This lower limit will give lower clamping forces and thus be on the safe side. A more realistic value may be calculated for average normal stress under the relaxation process ($N_1-0.5\Delta N$) and was used in the analysis. This implies that Eq. 4-8 is revised into Eq. 4-9 for clamping forces.

$$H_2 = \frac{(N_1 - 0.5\Delta N)}{\cos \theta} \quad 4-9$$

Barton and Choubey's equation, Eq. 4-10, of joint shear stiffness is based on experimental measurements and assumes that peak shear displacement is equal to 1% of the joint length (L). The joint peak shear displacement for a novel block size (3-12 m) is lower than 1% and is between 0.13% and 0.58%, with an average of 0.35% according to Barton and Bandis (1982). Therefore, instead of assuming joint peak shear displacement equal to 1% of

the joint length, a joint length of 0.35% is applied, and Eq. 4-10 is revised as Eq. 4-11. For a block with a fixed block base, the joint length can be calculated based on the block base and half-apical angle.

$$k_s = \frac{100}{L} \sigma_n \tan \varphi = \frac{100}{L} \left(\frac{N_1 - 0.5\Delta N}{L} \right) \tan \varphi \quad 4-10$$

$$k_s = \frac{100}{0.35L} \sigma_n \tan \varphi = \frac{100}{0.35L} \left(\frac{N_1 - 0.5\Delta N}{L} \right) \tan \varphi \quad 4-11$$

Substitution of Eq. 4-11 into Eq. 3-4 gives Eq. 4-12. Note that the unit of joint stiffness in Eq. 4-11 is MPa/m, and joint stiffness in Eq. 3-4 has the unit of MN/m. Therefore Eq. 4-11 must be multiplied by the joint area, which is the joint length multiplied by 1, unit length.

$$\Delta N = \frac{\frac{N_1}{L} \frac{100}{0.35L} \left(\frac{N_1 - 0.5\Delta N}{L} \right) \tan^2 \theta + \frac{N_1}{RL} \frac{100}{0.35L} \left(\frac{N_1 - 0.5\Delta N}{L} \right) \tan \varphi}{\tan^2 \theta \left(\frac{1}{K_{s,R}} + \frac{1}{L \frac{100}{0.35L} \left(\frac{N_1 - 0.5\Delta N}{L} \right) \tan \varphi} \right) + \frac{1}{K_{N,R}} + \frac{1}{RL \frac{100}{0.35L} \left(\frac{N_1 - 0.5\Delta N}{L} \right) \tan \varphi}} \quad 4-12$$

4.3.3 Ratio of joint stiffness

The ratio of joint normal stiffness to joint shear stiffness (R) depends on the normal stress, σ_n (Bandis, 1983); the mathematical relation will be described below. Even for this case, it is anticipated that the average normal stress will best reflect the situation.

$$R = A \sigma_n^{-0.595} = A \left(\frac{N_1 - 0.5\Delta N}{L} \right)^{-0.595} \quad 4-13$$

A values between 4.5 and 15.8 cover the area observed by Bandis. Substitution of Eq. 4-13 into Eq. 4-12 gives Eq. 4-14, which is used to estimate normal force reduction. ΔN exists in both sides of Eq. 4-14, which cannot be solved explicitly. Therefore, an implicit solution must be applied.

$$\Delta N = \frac{\frac{N_I}{L \frac{100}{0.35L} \left(\frac{N_I - 0.5 \times \Delta N}{L} \right) \tan \varphi} \tan^2 \theta + \frac{N_I}{A \left(\frac{N_I - 0.5 \times \Delta N}{L} \right)^{-0.595} L \frac{100}{0.35L} \left(\frac{N_I - 0.5 \times \Delta N}{L} \right) \tan \varphi}}{\tan^2 \theta \left[\frac{1}{K_{s,R}} + \frac{1}{L \frac{100}{0.35L} \left(\frac{N_I - 0.5 \times \Delta N}{L} \right) \tan \varphi} \right] + \frac{1}{K_{N,R}} + \frac{1}{A \left(\frac{N_I - 0.5 \times \Delta N}{L} \right)^{-0.595} L \frac{100}{0.35L} \left(\frac{N_I - 0.5 \times \Delta N}{L} \right) \tan \varphi}} \quad 4-14$$

4.3.4 Summary of ultimate limit state function and its variables

- *Ultimate state function*

The ultimate limit state function for block stability is a complex function and contains interactions between numerous geometrical and mechanical parameters.

- *Variables*

Limit state function (Eq. 4-14 and 4-4) include both random and deterministic variables. Random variables in the limit state function are normal force, normal force reduction, the joint friction angle, the half-apical angle, the stiffness ratio coefficient and model uncertainty. Some of the random variables in the equations mentioned are determined directly from field investigations, such as the half-apical angle, the joint friction angle and the stiffness ratio coefficient, or are based on the literature, such as model uncertainty. Others are estimated indirectly by equations such as normal

force and normal force reduction. N_1 (normal force from induced stress) is a function of horizontal stress and the half-apical angle and can be obtained from Kirsch's (1898) equation.

Deterministic variables are those that have a fixed value in a reliability analysis. In the limit state function mentioned above, γ_w (unit weight density), $K_{N,R}$ (normal surrounding rock stiffness) and $K_{S,R}$ (shear surrounding rock stiffness) were treated as deterministic variables. The unit weight density was assumed to have a deterministic value equal to 0.027 MN/m^3 .

The values of $K_{S,R}$ and $K_{N,R}$ are calculated for typical hard rock ($E=60 \text{ GPa}$) and different half-apical angles. The variation in $K_{N,R}$ and $K_{S,R}$ for each range of half-apical angles is about 10%. There is limited influence in determining normal force reduction, and the variation in each range of half-apical angles was ignored to facilitate calculation.

4.4 FORM analysis

4.4.1 Inputs

- *Coefficient A*

As mentioned earlier, A varies between 4.5 and 15.8 and is assumed to have a uniform distribution.

- *Friction angle*

Based on the literature for jointed hard rock (SKB, 2009), the friction angle was considered to be normally distributed 37 ± 3 degrees. Friction angle was considered with more variation (37 ± 5.5 degrees) to study the influence of friction angle dispersion.

- *Half-apical angle*

The half-apical angle is reported to have a normal distribution. The coefficient of variation of the half-apical angle varies between 13% and 55% (Call, 1992).

- *Model uncertainty*

The uncertainty of the analytical solution was discussed and described in Chapter 3. The distribution for model uncertainty has been approximated to be normal distribution with a mean value of 0.81 and standard deviation of 0.125.

- *Normal force*

Normal force due to induced stress is a random variable in the limit state function. Normal force is a function of horizontal stress, vertical stress and the half-apical angle. Distribution for normal force on the joint plane (N_1) can be obtained by using Monte Carlo simulations for the Kirsch equations to assess induced stress in radial and tangential directions, after which these stresses are transformed in the direction of the normal joint plane. Finally the normal force which is the product of normal stress and joint area could be calculated for each Monte Carlo simulation. Best fit has been applied to find the distribution parameter, mean and standard deviation, for normal or log normal distribution in order to use them in the calculations.

- *Vertical stress*

The vertical stress was reported in Brown and Hoek (1980) and Sugawara and Obara (1993) as $0.027z$ (MPa), where z is the depth. Depth was considered as 500 m.

- *Horizontal stress*

Among Fennoscandia cases in which the maximum horizontal stresses exceed the vertical stress (Stephansson, 1993), a case from Äspö, Sweden (SKB, 2009), was selected. Equations for major and minor stresses to estimate horizontal stresses are presented in Table 4-1. The equation for minor horizontal stress was selected since minor stresses are more critical to block stability.

The accuracy of stress measurement depends on three factors – natural uncertainty, measurement uncertainty and data analysis uncertainty (Amadei and Stephansson, 1997). The expected uncertainty for the stress measurement could be 10-20% (Gonano and Sharp, 1983; Herget, 1986; Pine and Kwakwa, 1989; Haimson, 1990).

Table 4-1. Normal distribution parameters for horizontal stress models from Äspö (SKB, 2009)

Parameter	Mean value MPa	Coefficient of variation
Major horizontal stress (MPa)	$0.039z+3$	12%
Minor horizontal stress (MPa)	$0.022z+1$	13%

- *Normal force reduction*

Eq. 4-14 describes the relationship of angles (half-apical angle and joint friction angle) and normal force to the estimated normal force reduction. The distribution for normal force reduction is calculated based on a Monte

Carlo random generation of horizontal stress, the joint friction angle, the half-apical angle, the stiffness ratio coefficient and an iteration process to implicitly solve Eq. 4-14. Table 4-2 shows the calculation process for calculating the distribution for normal force reduction based on a Monte Carlo simulation. A distribution using a goodness test could be fitted into ΔN . The significance level was set at 1%. To perform the process, a code in Matlab was written and used.

Table 4-2. The process order to assess distribution for normal force reduction

Order	Process
1	Random selection using Monte Carlo for σ_h
2	Random selection using Monte Carlo for θ
3	Closed form solution (Kirsch solution)
4	Stress transformation and force calculation
5	Calculation of N_1
6	Choosing $K_{N,R}$ and $K_{S,R}$ according to half-apical angle
7	Random selection using Monte Carlo for ϕ
8	<p>Iteration process for ΔN, until $\Delta N_i = \Delta N_{i+1}$</p> $\Delta N = \frac{\frac{N_1}{L \frac{100}{0.35L} \left(\frac{N_1 - 0.5\Delta N}{L} \right) \tan \phi} \tan^2 \theta + \frac{N_1}{A \left(\frac{N_1 - 0.5\Delta N}{L} \right)^{-0.595} L \frac{100}{0.35L} \left(\frac{N_1 - 0.5\Delta N}{L} \right) \tan \phi}}{\tan^2 \theta \left(\frac{1}{K_{S,R}} + \frac{1}{L \frac{100}{0.35L} \left(\frac{N_1 - 0.5\Delta N}{L} \right) \tan \phi} \right) + \frac{1}{K_{N,R}} + \frac{1}{A \left(\frac{N_1 - 0.5\Delta N}{L} \right)^{-0.595} L \frac{100}{0.35L} \left(\frac{N_1 - 0.5\Delta N}{L} \right) \tan \phi}}$ $\Delta S = \Delta N \times \tan \theta$
9	Best fitting to find normal or log normal distribution parameters for ΔN

4.4.2 Correlation coefficient

Some of the random variables such as the forces are correlated with one another and the angles. The correlation coefficient between variables is calculated based on Eq. 4-15.

$$r = \frac{\sum_{i=1}^n (X_i - \bar{X})(Y_i - \bar{Y})}{\sigma_X \sigma_Y} = \frac{E[(X - \mu_X)(Y - \mu_Y)]}{\sigma_X \sigma_Y} \quad 4-15$$

The correlations between normal force and the half-apical angle, normal force reduction and the half-apical angle, and finally normal force reduction and the joint friction angle were considered.

4.5 Results and summary of FORM analyses

4.5.1 Introduction

Two groups were analysed to assess the sensitivity factors. The analyses in the first group were carried out to study the influence of half-apical angle dispersion (10-55%) on the sensitivity factors for dispersion of joint friction angle equal to 9%. The second group was studied for the influence of joint friction angle dispersion on the sensitivity factors. The same analyses of group one were performed but with dispersion of friction angle equal to 15%.

4.5.2 Critical sensitivity factors

Sensitivity factors may vary for different loading conditions and parameter values. A critical sensitivity factor is defined as the lowest value for the resistance variables and the highest value for the load variables.

The sensitivity factors for different coefficients of variation of the half-apical angle were calculated. A negative sign for the sensitivity factor indicates that the parameter is on the resistance side.

In the analyses, it was found that by having variation in a joint friction angle more than 15%, the most sensitive parameter is the joint friction angle.

The half-apical angle has two roles in the analyses. First, it influences the amount of normal force, which is resistance, and second, it determines the block volume and weight, which is the load. Being on both sides, the resistance and load, makes the half-apical angle a complex parameter in the analysis.

Based on the cases analysed in which the coefficient of variation of the half-apical angle is less than 15% and that of the joint friction angle less than 15%, the only critical sensitivity factor that is not close to zero belongs to model uncertainty, with a sensitivity factor of -1.

The most critical sensitivity factor for the case in which the half-apical angle has dispersion less than 15% and the joint friction angle has dispersion more than 15%, is the joint friction angle with sensitivity of close to -1. Other parameters have lower sensitivity. Table 4-3 summaries the critical sensitivity factors.

Table 4-3. Critical sensitivity factors

Coefficient of variation for angles	α_{N1}	$\alpha_{\Delta N}$	α_A	α_θ	α_φ	α_M
$Cov\theta \leq 15\%$ $Cov\varphi \leq 15\%$	0	0	0	0	0	-1.0
$Cov\theta \leq 15\%$ $Cov\varphi > 15\%$	-0.23	-0.20	0	-0.23	-0.95	-0.06
$Cov\theta > 15\%$	-0.68	-0.66	0.06	-0.43	-0.98	-0.11

If the block is fully unloaded ($N_1 = \Delta N$), there is no contribution from clamping forces. The ultimate limit state function can then be simplified to include only required rock bolts and block weight (see Eq. 4-3). Since a rock bolt has a lower uncertainty than geomaterial, in this limit state function, it was considered to be a deterministic value, and the only random variable is the half-apical angle. The FORM analyses show that, in this case, the sensitivity factor for the half-apical angle is equal to -1.

4.6 Comparison between partial factors and FORM

4.6.1 Partial factors and their application

The partial factors are calculated and the design values are applied in a limit state function (Eq. 4-3) to check the stability of the block and determine the support required to achieve a desirable safety index. The required rock support from partial factors was compared to that calculated using FORM.

If the characteristic values for normal force and normal force reduction are close to each other, then the sensitivity factor of the half-apical angle is set

to -1 and the design value for the block weight is calculated based on that. The design value for a rock bolt is calculated based on Eq. 4-3. Since deep tunnels usually have high in-situ stresses, loose blocks are rare (Li, 2010). An example for a shallow depth is described below.

4.6.2 Partial factors for a shallow depth tunnel

The mean value of the half-apical angle was considered equal to 15 degrees, and different values for the coefficient of variation of the half-apical angle were considered. Major stress at a depth of 30 m, as described in Table 4-1, was considered.

Table 4-4 shows the partial factors, design values, weight of the block and required rock support using the sensitivity factors proposed in Table 4-3 for a case with a 5% coefficient of variation in the half-apical angle. A FORM analysis was performed for this case, and FORM predicts the required rock support equal to 0.1 MN. In the table, V is the coefficient of variation, α is the sensitivity factor, β is the safety index and γ is the partial factor.

Table 4-4. Coefficient of variation, sensitivity, partial factors and design values
(Cov θ =5%)

Parameter	Mean	V	α	β t	γ	Design value
N (MN)	11.09	0.09	0	3	1	11.09
ΔN (MN)	10.59	0.09	0	3	1	10.59
A	A=4.5, B=15.86	0.32	0	3	1	10.18
Φ (degree)	50	0.10	0	3	1	50
θ (degree)	15	0.05	0	3	1	15
Model uncertainty	0.81	0.15	-1	3	1.85	0.43
Weight (MN)						0.2
Required rock bolt (MN)						0.1

For another case with a 10% coefficient of variation in the half-apical angle, the calculation was repeated. The results are presented in Table 4-5. FORM predicts the required rock bolt, 0.1 MN.

Table 4-5. Partial factors and design values for COV =10% of the half-apical angle

Parameter	Mean	V	α	β_t	γ	Design value
N (MN)	11.12	0.1	0	3	1	11.09
ΔN (MN)	10.65	0.1	0	3	1	10.65
A	10.18	0.32	0	3	1	10.18
Φ (degree)	50	0.10	0	3	1	50
θ (degree)	15	0.1	0	3	1	15
Model uncertainty	0.81	0.15	-1	3	1.85	0.43
Weight(MN)						0.2
Required rock bolt (MN)						0.1

For a case with uncertainty in the half-apical angle of 25%, the calculations were performed and the results are shown in Table 4-6. For this case, FORM predicts required rock support equal to 0.35 MN.

Table 4-6. Partial factors and design values for a COV =25% of the half-apical angle

Parameter	Mean	V	α	β_t	γ	Design value
N (MN)	11.48	0.16	-0.68	3	1.4	8.2
ΔN (MN)	10.98	0.16	-0.66	3	1.39	7.89
A	10.18	0.32	0.06	3	1.05	10.38
Φ (degree)	50	0.10	-0.98	3	1.34	37.31
θ (degree)	15	0.25	-0.43	3	1.42	10.56
Model uncertainty	0.81	0.15	-0.11	3	1.06	0.76
Weight (MN)						0.3
Required rock bolt (MN)						0.17

Another case was considered with 45% uncertainty. The calculations show that, based on a partial factor design, a rock bolt of 0.52 MN is required (see Table 4-7). As is shown in the table, the design value of normal force reduction is more than the normal force, which means that the resistance force in the limit state equation is zero. Therefore, the entire block weight must be supported. A FORM analysis shows that, in order to reach a safety index of 3, a bolt of 0.58 MN is required.

Table 4-7. Partial factors and design values for a COV =45% of the half-apical angle

Parameter	Mean	V	α	β_t	γ	Design value
N (MN)	13.28	0.62	-0.68	3	4.16	3.19
ΔN (MN)	12.68	0.41	-0.66	3	2.43	5.21
A	10.18	0.32	0.06	3	1.05	10.38
Φ (degree)	50	0.10	-0.98	3	1.34	37.31
θ (degree)	15	0.45	-0.43	3	2.38	6.30
Model uncertainty	0.81	0.15	-0.11	3	1.06	0.79
Weight (MN)						0.52
Required rock bolt (MN)						0.52

4.7 Discussion and conclusion

The influences of parameter uncertainties together with model uncertainty on the design of rock support of a block were analysed.

Dispersion of the half-apical angle, in other words, the dispersion of the joint dip angle, is the dominant parameter. If the dispersion of the joint dip angle is less than 15%, then friction or model uncertainty is the most sensitive parameter, depending on the coefficient of variation of the friction angle.

For tunnels that are subject to full unloading of the blocks, there is only one sensitive parameter, which is the half-apical angle.

The comparison shows that the partial factors as well as a FORM analysis can be used for cases with a low uncertainty in the half-apical angle.

By increasing the dispersion of the joint dip angle, the partial factors for the forces are increased and become large. Therefore, the design value of normal force reduction becomes equal to the normal force, which corresponds to the case where clamping forces are ignored. However, for cases in which the joint dip angle has low dispersion, ignoring clamping forces leads to an uneconomical design. For random joint sets with a large coefficient of variation of the joint dip angle, the partial factors are not applicable.

The examples show that the required rock support increases dramatically when the dispersion of the joint dip angle increases. The costs of overdesign can be compared to those of collecting more precise data for the joint dip angle and applying the observational method.

The half-apical angle has a dual function in the safety margin. The half-apical angle determines the forces (normal and normal reduction) on the block, which are the resistance, and also has a direct influence on the weight of block, which is the load in a limit state function. This makes the application of partial factors difficult for a block stability analysis.

It may be possible to apply partial factors to the block stability in some circumstances such as a low coefficient of variation of the half-apical angle. It seems, however, that a FORM analysis is in general preferable.

Chapter 5 Discussion and conclusion

5.1 Introduction

The theories for analysing block stability and a new model for such were described in the previous chapters. This chapter provides a summary and conclusions with an emphasis on the practical perspective to both researchers and designers.

5.2 Summary

There are different design tools available for block stability analysis such as kinematic limit equilibrium (KLE), DFN-DEM and analytical solutions. In this thesis, different approaches of the most frequently applied method, KLE, were compared with more advanced DFN-DEM methods. The results of the two approaches differ widely. In many cases, kinematic limit equilibrium approaches provide uneconomical or unsafe design. This is due to the assumptions in both estimating block volume and analysing the equilibrium of the blocks.

Numerical discrete models, like DEM, have potential to give results close to reality, but these models cannot provide a detailed description of the mechanism of failure and also have limitations in applying a reliability analysis. Comparing results of numerical and analytical solutions reveals that a key stage was ignored in the analytical solution proposed by Crawford and Bray. A comparison of analytical and numerical solutions leads to a better understanding of the failure mechanism and, based on this, a conceptual model is proposed. The new conceptual model provides a description of how the clamping forces develop. The relaxation of induced stresses is quantified using the conceptual model. They are a function of

joint stiffness, the modulus of the surrounding rock and the apical angle of the block.

More numerical models were run to study the initial of the clamping forces, and it was determined that acting local stresses, which are proportional to joint stiffness, block configuration and the regional stress field are important.

The model uncertainty of the new solution was quantified by comparing the results from the analytical models to those from DEM. The accuracy of the new analytical solution is acceptable.

Further studies were performed to assess sensitivity factors and study the applicability of partial factors to block stability. Based on the complex equation of the safety margin, FORM analyses were performed and the sensitivity factors were assessed. It was observed that the sensitivity factors depend on the uncertainty of the apical angle and friction angle. Sensitivity factors change from one case to another. The critical sensitivity factors were proposed, and some cases were estimated based on the required rock support. It was observed that the required rock support depends significantly on uncertainties of the apical angle and that the use of partial factors is questionable in designing the rock support for blocks in tunnels.

5.3 Conclusion

Block failure is a complex problem although it seems to be a simple failure mode. Today's design methods, such as kinematic limit equilibrium, produce questionable results due to their simplifications.

Block stability is governed by clamping forces, which are a result of a complex mechanism and interaction between many parameters, some of which are not well known. Simple mechanisms for estimating clamping forces such as Crawford-Bray or those based on continuum mechanics are mostly on the unsafe side of design. The results of the methods noted, such as Crawford-Bray, are questionable and have a limited validity range only for stiff joints.

The new analytical solution considers the complex interaction and relaxation of clamping forces due to the existence of joints. This has acceptable model uncertainty compared to previous solutions and suggests that an incomplete understanding of the failure mechanism is the main source of model uncertainty in the analytical solution. A complete understanding of the failure mechanism is therefore vital.

In addition to the relaxation of induced stress, the relaxation of regional stress before excavation is a key issue in analysing block stability. Clamping forces on a single block in a massive rock mass are lower than clamping forces on a corresponding block in blocky ground for the same given in-situ stresses and stiffness properties.

The relevant sensitivity factors calculated using FORM differ from one case to another based on the uncertainties of the apical angle and friction angle. The use of partial factors is uncertain. Partial factors may be applied in some circumstances but are not always applicable, and a FORM analysis is preferable.

The fracture dip angle governs the sensitivity factors for a reliability analysis. The more uncertain the half-apical angle, the more rock support is

required. The costs of gathering information ought to be compared to the costs of overdesign.

5.4 Suggestions to the designer

The designer must decide which design tool to use for determining stability and the required rock support for a block. The key is to realise the weakness of each design tool. A complete understanding of the failure mechanism is often vital and has to be compared with the prerequisites of existing models. Considering a single block in massive rock is on the safe side.

Taking clamping forces into consideration in the design of blocks, or not, depends on the uncertainties in the dip angle of joints. If there is great uncertainty in the dip angle, partial factors for normal force and normal force reduction will be high and design clamping forces will be close to zero. The costs of overdesign must be compared with the costs of gathering more information about the joint dip angle (apical angle).

Based on the limitations of partial factors, it is recommended that a FORM analysis be performed for a reliability analysis.

5.5 Further research

In order to confirm the conclusions given above, further calculations for different cases ought to be performed. Because of the complex interactions, more knowledge is required about the shear and normal stiffness of joints and how the stiffnesses depend on the normal stress and scale. Assumptions in in-situ stress conditions and about the symmetric form of a block place limitations on the applicability of the solution. Based on the conceptual model discussed here, the solution can be developed into more general cases for asymmetric and inclined in-situ stress.

References

1. Amadei B. Stephansson O. 1977, *Rock stress and its measurement*, Chapman & Hall
2. Bagheri M. 2009, Model uncertainty of design tools to analyze block stability, licentiate thesis, Royal Institute of Technology
3. Barton, N. Bandis, S. 1982, Effects of block size on the shear behaviour of jointed rock. Keynote Lecture, *23rd US Symposium on Rock Mechanics*, Berkeley, California
4. Bandis S.C. Lumsden A.C. Barton N. R. 1983, Fundamentals of rock joint deformation, *Int. J. Rock Mech. Min. Sci. & Geomech. Abstr.* 20(6), pp 249-268
5. Barton N. Choubey V. 1977, The shear strength of rock joints in theory and practice, *Rock Mechanics and Rock Engineering*, 10, pp 1-54
6. Batschelet E. 1981, *Circular statistics in biology*, 1st Ed. New York: Academic Press
7. Benedik R. 1987, Maintenance of tailrace tunnel at Järsjöströmmen water power plant, in *Bergmekanikdagen*, pp 93-105
8. Berglund J. 2001, Clab2 etapp 2 Byggnadsgeologisk dokumentation, SKB, Report number 0519001-045
9. Bergman S. 1985, *Twenty years of Swedish rock mechanics R&D*, pp 23-35
10. Call R.D. 1992, Slope stability, in *SME mining engineering handbook*, 2nd Edition, Vol. 1, Senior Editor Howard L. Hartman, Port City Press, Baltimore USA. pp 881-896

11. Chan H.C. Einstein H. 1981, Approach to complete limit equilibrium analysis for rock wedges: The method of “artificial supports”, *Rock Mechanics and Rock Engineering* 14, 59-86
12. Crawford A.M. Bray J.W. 1983, Influence of in-situ stress field and joint stiffness on rock wedge stability in underground openings, *Can Geotech. J.* 20, pp 1990-2001
13. Cundall P. 1971, A computer model for simulating progressive large scale movements in blocky rock system. In: *Proc., Intern. Soc. of Rock Mechanics*, Nancy, Vol. 1
14. Curran J.H. Corkum B. and Hammah R.E. 2004, three dimensional analysis of underground wedges under the influence of stresses, in *Proc. Gulf Rock 04 conf.* Elsevier Science Publisher.
15. Dershowitz W.S. Einstein H. 1988, Characterizing rock joint geometry with joint system models. *Rock Mech. and Rock Engn.*, Vol. 21, pp 21-51
16. Ditlevsen O. 1982, Model uncertainty in structural reliability, *Structural Safety J.* 1(1) 73-86
17. Dinis C. 1977, Computer model for block size analysis of jointed rock masses, *Proc. 15th APCOM. Brisbane, Australia*, pp 305-315
18. Diederichs M.S. Espley C. Langille, Hutchinson D.J. 2000, A semi-empirical hazard assessment approach to wedge instability in underground mine openings, In *GeoEng*, Melbourne, CD-ROM
19. Duncan J.M. 1992, State-of-the-art: Static stability and deformation analysis, *Proc., Stability and Perf. of Slopes and Embankments-II*, ASCE, Reston, Va. 1, 222-266
20. Elsworth D. 1986, Wedge stability in the roof of a circular tunnel: plane strain condition, *Int. J. Rock Mechanics and Mining Sci. & Geomech*,

- Abs, 23(2), pp 177-81
21. Eurocode 1997-1:2004. *Eurocode 7: Geotechnical design – Part 1: General rules*. European Committee for Standardization
 22. Fredriksson A. Hässler L. Söderberg L. 2001, Extension of CLAB, numerical modeling, deformation measurements and comparison of forecast with outcome, *Rock Mechanics a challenge for society*, Särkkä & Eloranta (Ed.), Swets&Zeitlinger Lisse pp 743-747
 23. Goodman R. Shi G.H. 1982, Calculation of support for hard, jointed rock using the keyblock principle, *PROC. 23RD US Symposium on Rock Mechanics*, pp 883-893, California
 24. Goodman R. Shi. G.H. 1985, *Block theory and its application to rock engineering*. 1st Ed. London: Prentice-Hall
 25. Goodman, R. 1989, *Introduction to the rock mechanics*, 2nd Ed, New York: John Wiley and Sons
 26. Gonano L.P. and Sharp, J.C. 1983, Critical evaluation of rock behaviour for in-situ stress determination using the overcoring method, in *Proc. 5th Cong. Int. Soc. Rock Mech. (ISRM)*, Melbourne, Balkema, Rotterdam, pp A241-50
 27. Hadjigeorgiou J. Grenon M. 2005, Rock slope analysis using fracture systems, *Int. J. of Surface Mining, Reclamation and Environment*, 19 (2), pp 87-99
 28. Haimson B.C. 1990, Stress measurements in the Sioux falls quartzite and the state of stress in the Midcontinent, in *Proc. 31st US symposium Rock Mech.*, Golden, Balkema, Rotterdam, pp 3976-404
 29. Hansen L. Martna J. 1989, Engineering geology of a large tunnel at the Vargöns hydropower station, Sweden, *Bergmekanikdagen*, pp77-96

30. Hedlund B. 1980, Rockslide in the Harsprånget No.5 tailrace tunnel, *Bergmekanikdagen*, pp 209-238
31. Herget G. 1986, Changes of ground stresses with depth in the Canadian shield, in *Proc. Int. Symp. on Rock Stress and Rock Stress Measurements*, Stockholm, Centek Publ. Luleå, pp 61-8
32. Hoek E. and Brown, E.T. 1980, *Underground excavations in rock*. London: Instn Min. Metall.
33. Honjo Y. Kieu Le and Hara T. 2009, Code calibration in reliability based design level I verification format for geotechnical structures, in *Geotechnical Risk and Safety*, pp 435-452
34. ISRM International Society for Rock Mechanics, Commission on Standardization of Laboratory and Field Test. 1978, Suggested methods for the quantitative description of discontinuities in rock masses, *Int. J. Rock Mechanics & Mining Sci.* Vol. 15 pp 319-68
35. Jing L. Nordlund E. Stephansson O. 1992, An experimental study on the anisotropy and stress dependency of the strength and deformability of rock joints, *Int. J. Rock Mech. Min Sci. & Geomech.* Vol. 29(6), pp 535-542
36. Kemeny D.J.M.A. Hagaman R.M. and Wu X. 1993, Analysis of rock fragmentation using digital image processing *J. Geotech. Engng* 199, pp 1144-1160
37. Kim B.H. Cai M. Kaiser P.K. and Yang H.S. 2007, Estimation of block sizes for rock masses with non-persistent joints, *Rock Mech. Rock Engng.* 40 (2), pp 169–192
38. Kirch G. 1898, Die theorie der elastizität und die bedurfnisse der festigkeitslehre. *Zeitschrift des Vereines Deutscher Ingenieure*; Vol. 42:797–807.

39. Kleine T. 1988, A mathematical model of rock breakage by blasting, PhD thesis, Uni. Of Queensland, Australia
40. Krauland N. 1975, Deformation around a cut and fill slope-experiences derived from in situ observation, *Bergmekanikdagen*, pp 202-216
41. Li C.C. 2011, Field observations of rock bolts in high stress rock masses, *Rock Mech. Rock Engng.* 43 (4), pp 491–6
42. Mardia K.V. 1972, *Statistics of Directional Data*. 1st Ed. London: Academic Press
43. Mauldon M. Zhao M. 1995, Stability of key blocks under self-weight and surface forces, *Proc. 35th US. Symposium on Rock Mech.* pp 113-118
44. Morfeldt C. 1973, Bergrums Förstärkning och tätning vid lagring av varma och kalla media, *Bergmekanikdagen*, PP 257-268
45. Nomikos P.P. Soianos A.I. Tsoutrelis C.E. 1999, Stability of symmetric wedge formed in the roof of a circular tunnel: non-hydrostatic natural stress field, *Int. J. Rock Mech. & Mining Sci.* 36, pp 687-691
46. Nomikos P.P. Soianos A.I. Tsoutrelis C.E. 2002, Symmetric wedge in the roof of a tunnel excavated in an inclined stress field, *Int. J. Rock Mech., & Min. Sci.* 39, pp 59-67
47. Nomikos P.P. Yiouta –Mitra P.V. Soianos A.I. 2006, Stability of asymmetric roof wedge under non-symmetric loading, *Rock Mech, Rock Engng*, 39 (2), pp 121-129
48. Nomikos P.P. Sofianos A.I. 2008, Progressive failure of 2D symmetric roof rock wedges, *5th Asian Rock Mechanics Symposium*, Tehran
49. Oda M. Yamabe T. Ishizuka Y. Kumasaka H. Tada H. and Kimura K. 1993, Elastic stress and strain in jointed rock masses by means of crack tensor analysis, *Rock Mech. Rock Engng.* 26 (2), pp 89-112

50. Olsson P. Stille H. 1989, Conversion of oil cavern to coal storage, *BeFo Bergmekanikdagen*, pp 181-193
51. Palmstorm A. 2005, Measurements of and correlations between block size and rock quality designation (RQD), *Tunnel and Underground Space Technology*, Vol. 20(4), pp 362-377
52. Pine R.J. Kwakwa K.A. 1989, Experience with hydrofracture stress measurements to depth of 2.6km and implications for measurements to 6km in Carnmenellis granite, *Int. J. Rock Mech. Min. Sci. & Geomech Abst.* 16, pp 565-71
53. Sjöström Ö. 1989, Tunnel construction in difficult rock, Mtera hydro power plant, Tanzania, *Bergmekanikdagen*, pp 243-255
54. SKB, 2009, Site description of Laxemar at completion of the site investigation phase SDM-Site Laxemar, SKB
55. Sofianos A.I. 1984, Numerical simulation of underground excavations within jointed rock of infinite extent, PhD thesis, Uni, of London
56. Sofianos A.I. 1986, Stability of Rock Wedges in Tunnel Roofs, *In. J. Rock Mech. Min. Sci. & Geomech. Abst.*, Vol. 23(2), pp, 119-130
57. Stark T. Eid H. 1998, Performance of three-dimensional slope stability methods in practice, *Journal of Geotechnical and Geoenvironmental Engineering*, Vol. 124(11), pp 1049-1060
58. Starzec P. Anderson J. 2002, Application of two level factorial design to sensitivity analysis of key block statistics from fracture geometry In *J. Rock Mechanics and Mining Sciences*, 39 pp 234-255
59. Stephansson O. 1993, Rock stress in the Fennoscandian shield, in *Comprehensive Rock Engineering* (ed. J.A. Hudson), Pergamon Press, Oxford, Chapter 17, Vol. 3, pp 445-59
60. Sugawara K. Obara Y. 1993, Measuring rock stress, in *Comprehensive*

- Rock Engineering* (Ed. J.A. Hudson), Pergamon Press Oxford, Chapter 21, Vol. 3, pp 533-52
61. Sundel BO. 1991, Rehabilitation of the tunnels in the Tåsan hydropower station, *BeFo Bergmekaniksdagen*, pp 95-113
62. Villaescusa E. Brown E.T. 1991, Stereological estimation of in-situ block size distributions, In *Proceedings of 7th Congress, ISRM Aachen*, Ed. W. Wittke Vol. 1. pp 361-365. Balkema. Rotterdam
63. Åkesson J. 1985, The biggest underground store for crude oil in the world. Experiences from rock construction in Korea, *Bergmekaniksdagen*, pp 209-225